

Schwaab, Bernd; Zhang, Xin; Lucas, André

Working Paper

Modeling extreme events: Time-varying extreme tail shape

Sveriges Riksbank Working Paper Series, No. 399

Provided in Cooperation with:

Central Bank of Sweden, Stockholm

Suggested Citation: Schwaab, Bernd; Zhang, Xin; Lucas, André (2020) : Modeling extreme events: Time-varying extreme tail shape, Sveriges Riksbank Working Paper Series, No. 399, Sveriges Riksbank, Stockholm

This Version is available at:

<https://hdl.handle.net/10419/232602>

Standard-Nutzungsbedingungen:

Die Dokumente auf EconStor dürfen zu eigenen wissenschaftlichen Zwecken und zum Privatgebrauch gespeichert und kopiert werden.

Sie dürfen die Dokumente nicht für öffentliche oder kommerzielle Zwecke vervielfältigen, öffentlich ausstellen, öffentlich zugänglich machen, vertreiben oder anderweitig nutzen.

Sofern die Verfasser die Dokumente unter Open-Content-Lizenzen (insbesondere CC-Lizenzen) zur Verfügung gestellt haben sollten, gelten abweichend von diesen Nutzungsbedingungen die in der dort genannten Lizenz gewährten Nutzungsrechte.

Terms of use:

Documents in EconStor may be saved and copied for your personal and scholarly purposes.

You are not to copy documents for public or commercial purposes, to exhibit the documents publicly, to make them publicly available on the internet, or to distribute or otherwise use the documents in public.

If the documents have been made available under an Open Content Licence (especially Creative Commons Licences), you may exercise further usage rights as specified in the indicated licence.

SVERIGES RIKSBANK
WORKING PAPER SERIES

399



Modeling extreme events: time-varying extreme tail shape

Bernd Schwaab, Xin Zhang and André Lucas

December 2020

WORKING PAPERS ARE OBTAINABLE FROM

www.riksbank.se/en/research

Sveriges Riksbank • SE-103 37 Stockholm

Fax international: +46 8 21 05 31

Telephone international: +46 8 787 00 00

The Working Paper series presents reports on matters in the sphere of activities of the Riksbank that are considered to be of interest to a wider public.

The papers are to be regarded as reports on ongoing studies and the authors will be pleased to receive comments.

The opinions expressed in this article are the sole responsibility of the author(s) and should not be interpreted as reflecting the views of Sveriges Riksbank.

Modeling extreme events: time-varying extreme tail shape*

Bernd Schwaab,^(a) Xin Zhang,^(b) André Lucas^(c)

^(a) European Central Bank, Financial Research

^(b) Sveriges Riksbank, Research Division

^(c) Vrije Universiteit Amsterdam and Tinbergen Institute

Sveriges Riksbank Working Paper Series

No. 399

Abstract

We propose a dynamic semi-parametric framework to study time variation in tail parameters. The framework builds on the Generalized Pareto Distribution (GPD) for modeling peaks over thresholds as in Extreme Value Theory, but casts the model in a conditional framework to allow for time-variation in the tail shape parameters. The score-driven updates used improve the expected Kullback-Leibler divergence between the model and the true data generating process on every step even if the GPD only fits approximately and the model is mis-specified, as will be the case in any finite sample. This is confirmed in simulations. Using the model, we find that Eurosystem sovereign bond purchases during the euro area sovereign debt crisis had a beneficial impact on extreme upper tail quantiles, leaning against the risk of extremely adverse market outcomes while active.

Keywords: dynamic tail risk, observation-driven models, extreme value theory, European Central Bank (ECB), Securities Markets Programme (SMP).

JEL classification: *C22, G11.*

*Author information: André Lucas, VU University Amsterdam, De Boelelaan 1105, 1081 HV Amsterdam, The Netherlands, Email: a.lucas@vu.nl. Bernd Schwaab, Financial Research, European Central Bank, Sonnemannstrasse 22, 60314 Frankfurt, Germany, email: bernd.schwaab@ecb.int. Xin Zhang, Research Division, Sveriges Riksbank, SE 103 37 Stockholm, Sweden, email: xin.zhang@riksbank.se. An earlier version of this paper was circulated as “Tail risk in government bond markets and ECB unconventional policies.” Schwaab thanks ECB DG-M for comments and access to high-frequency data on SMP bond purchases. The views expressed in this paper are those of the author and they do not necessarily reflect the views or policies of the European Central Bank or Sveriges Riksbank.

1 Introduction

This paper proposes a novel semi-parametric framework to study time variation in tail fatness for long univariate time series, applied to high-frequency government bond returns during times of unconventional central bank policies. The new method builds on ideas from Extreme Value Theory (EVT) by using a conditional Generalized Pareto Distribution (GPD) to approximate the tail beyond a given threshold, and endowing this conditional GPD distribution with time-varying parameters. The GPD is an appropriate tail approximation for most heavy-tailed densities used in econometrics and actuarial sciences; see, for example, [Embrechts et al. \(1997\)](#), [Coles \(2001\)](#), and [McNeil et al. \(2010, Chapter 7\)](#). As a result, the GPD plays a central role in the study of extremes, comparable to the role the normal distribution plays when studying observations in the center of the distribution. Our framework allows us to study the time-variation in tail parameters associated with time series observations from a wide class of heavy-tailed distributions; see [Rocco \(2014\)](#) for a recent survey of EVT methods in finance. We discuss the handling of non-tail time series observations, inference on deterministic and time-varying parameters, and ways to relate time-varying parameters to observed covariates. In this context we also study the effect of time-varying pre-filtering methods possibly applied to the data before the dynamic GPD model is fitted.

In our model, the time-varying tail shape and tail scale parameters of the GPD are driven by the score of the local (time t) objective function; see e.g. [Creal et al. \(2013\)](#) and [Harvey \(2013\)](#). In this approach, the time-varying parameters are perfectly predictable one step ahead. This makes the model observation-driven in the terminology of [Cox \(1981\)](#). The log-likelihood is known in closed form, facilitating parameter estimation and inference via standard maximum likelihood methods. Simulation evidence reveals that our model and estimation approach is able to recover the time-varying tail shape and tail scale parameters sufficiently accurately, as well as EVT-based market risk measures such as Value-at-Risk (VaR) and Expected Shortfall (ES) at high confidence levels (say, 99%). This is the case even if the model is misspecified or the GPD approximation is not exact. The latter is particularly important in our finite sample setting, where the limiting result of the GPD can

only hold approximately given the choice of a finite exceedance threshold in any particular sample.

We apply our modeling framework to study the location, scale, and upper tail impact of bond purchases undertaken by the Eurosystem – the European Central Bank (ECB) and its 17 national central banks at the time – during the euro area sovereign debt crisis between 2010 and 2012. We focus on bond purchases within the Eurosystem’s Securities Markets Programme (SMP), which targeted sovereign bonds of five euro area countries: Greece, Ireland, Italy, Portugal, and Spain. Based on high-frequency data for five-year benchmark bonds, and explicitly accounting for time-variation in fat tails, we find that purchases lowered the conditional location (mean) of future bond yields by up to -2.9 basis points (bps) per €1 bn of purchases. The impact estimates for the two largest SMP countries, Italy and Spain, are -1.5 bps and -2.6 bps per €1 bn of purchases, respectively. These impact estimates are marginally smaller in absolute value than earlier estimates based on different methodologies; see [Eser and Schwaab \(2016\)](#), [Ghysels et al. \(2017\)](#), and [Pooter et al. \(2018\)](#).

In addition, we find that SMP purchases had a beneficial impact on the extreme upper tail quantiles of yield changes. This suggests that central bank bond purchases lean against the risk of extremely adverse market outcomes while they are active. The beneficial impact is mostly explained by moving the center of the predictive distribution to the left and narrowing it. Beneficial secondary effects come about via the SMP’s effect on tail shape and tail scale for large economies such as Spain and Italy. The impact of purchases on tail quantiles is larger than their impact on the conditional location (mean). We estimate that the 97.5% VaR was reduced by 3.8, 6.0, 5.9, 2.1, and 6.9 bps per €1 bn Eurosystem intervention in Spanish, Greek, Irish, Italian, and Portuguese five-year benchmark bonds, respectively. The impact grows with the extremeness of the VaR. We estimate that the 99.5% VaR was reduced, respectively, by 5.1, 10.1, 12.5, 2.9, and 15.4 bps per €1 bn of Eurosystem purchases in the above bonds. The tail impact of the SMP purchases is economically relevant because extreme tail risks alone can force dealer banks and market makers to retreat from supplying liquidity to important segments of the sovereign bond market, particularly when their own VaR constraints are binding; see [Vayanos and Vila \(2009\)](#) and [Adrian and Shin \(2014\)](#). In

turn, malfunctioning sovereign bond markets can impair the transmission of the common monetary policy to all parts of the euro area. [Pelizzon et al. \(2013, 2016\)](#) provide evidence that market makers withdrew from trading Italian debt securities in 2011.

Our paper is related to at least two strands of literature: one on modeling time-variation in tail parameters and one on assessing the effectiveness of central bank unconventional monetary policy measures. Regarding the first, several papers propose methodology to study time variation in the tail index. [Davidson and Smith \(1990\)](#), [Coles \(2001, Chapter 5.3\)](#), and [Wang and Tsai \(2009\)](#), among others, also index the GPD tail parameters with time subscripts and equip them with a parameterized structure. Our approach is different in that their “tail index regression” approach requires conditioning variables that explain (all of) the tail variation. Such variables are not always available. By contrast, our “filtering approach” does not require such conditioning variables, and is arguably better suited for the real-time monitoring of extreme risks. Second, [Quintos et al. \(2001\)](#), [Einmahl et al. \(2016\)](#), [Hoga \(2017\)](#), and [Lin and Kao \(2018\)](#) derive formal tests for a structural break in the tail index. A number of subsequent studies applied such tests to financial time series data. [Werner and Upper \(2004\)](#) identify a break in the tail behavior of high-frequency German Bund future returns. [Galbraith and Zernov \(2004\)](#) argues that certain regulatory changes in U.S. equity markets have altered the tail index dynamics of equities returns, and [Wagner \(2005\)](#) demonstrates that changes in government bond yields appear to exhibit time-variation in the tail shape for both the U.S. and the euro area. [de Haan and Zhou \(2020\)](#) propose a non-parametric approach to estimating the extreme value index locally. Our paper adds to this strand of conditional EVT literature by proposing a model that allows us to study both the tail shape and tail scale dynamics directly in a semi-parametric way. Explanatory covariates can be included in the dynamics of both parameters, and likelihood ratio tests are available to test economically relevant hypotheses. Finally, unlike [Patton et al. \(2019\)](#), our tail VaR and ES dynamics explicitly account for fat tail shape beyond a threshold as emerging from EVT. The dynamics based on the score for the GPD contain weights for extreme observations. Such weights are absent in the elicitable score functions of [Patton et al.](#). The resulting dynamics in our model are, as a result, more robust, particularly for

the ES.

A second strand of literature assesses the impact of central bank asset purchases on bond yields and yield volatility. For example, [Ghysels et al. \(2017\)](#) study the yield impact of SMP bond purchases by considering bond yields and purchases at 15-minute intervals. In this way they mitigate a bias that unobserved factors could have introduced. The authors estimate that SMP interventions had an impact on the conditional mean of 10-year maturity bonds of between -0.2 and -4.2 bps per €1 bn of purchases. [Eser and Schwaab \(2016\)](#) study yield impact based on daily data. In their framework, identification is based on a panel model that exploits the cross-sectional dimension of the data. They find that, in addition to large announcement effects, purchases of 1/1000 of the respective outstanding debt had an impact of approximately -3 bps at the five-year maturity. [Pooter et al. \(2018\)](#) use the published weekly data of aggregate SMP purchases to test for an impact on country-specific sovereign bond liquidity premia. The authors find an average impact of -2.3 bps for purchases of 1/1000 of the outstanding debt. Our paper adds to the growing literature on assessing the effectiveness of central bank asset purchase programs by developing methodology for the extreme tail of the distribution.

Whereas [de Haan and Zhou \(2020\)](#) take a non-parametric perspective, the methodological part of this paper is closest to [Massacci \(2017\)](#), who also proposes a dynamic parametric model for the GPD parameters. Our framework is different in that we specify both parameters as functions of their respective scores, and adopt a non-diagonal scaling function. We cover inference on both deterministic and time-varying parameters, explain how to introduce additional conditioning variables, and provide Monte Carlo evidence. Owing to a novel autoregressive specification of the EVT threshold following [Patton et al. \(2019\)](#), our model can be fitted to both prefiltered and non-prefiltered time series data.¹

We proceed as follows. Section 2 presents our statistical model. Section 3 discusses our simulation results. Section 4 studies the tail impact of Eurosystem asset purchases. Section 5 concludes. A Web Appendix derives the score and scaling function for the tail shape model

¹For computer code and an enumeration of recent work on score-driven models see <http://www.gasmodel.com/code.htm>.

and provides further technical and empirical results.

2 Statistical model

2.1 Time-varying tail shape and scale

This section introduces our model with time-varying tail shape and tail scale for a univariate time series y_t , $t = 1, \dots, T$, where T denotes the number of observations. We assume

$$y_t = \mu_t + \sigma_t \varepsilon_t, \tag{1}$$

where $g(\varepsilon_t | \mathcal{F}_{t-1})$ is the conditional probability density function (pdf) of ε_t , μ_t and σ_t are the conditional location and scale of y_t , and $\mathcal{F}_{t-1} = \{y_{t-1}, y_{t-2}, \dots, y_1\}$ denotes the information set. The parameters μ_t and σ_t can take on many forms ranging from constant values to specifications with autoregressive and conditional volatility dynamics. Key, however, is that these parameters are typically mainly used to describe well the *center* of the distribution. In this paper, by contrast, we concentrate on the *tail* of the distribution using a dynamic extension of arguments from extreme value theory, similar to Patton's (2006) extension of copula theory to the dynamic, observation driven setting.

We assume the conditional pdf $g(\varepsilon_t | \mathcal{F}_{t-1})$ has heavy tails with time-varying tail index $\alpha_t > 0$. A prime example is the univariate Student's t distribution with $\nu_t = \alpha_t$ degrees of freedom. Other examples include the Pareto, inverse gamma, log-gamma, log-logistic, F , Fréchet, and Burr distribution with one or more time-varying shape parameters. Rather, however, than modeling the (dynamic) tail shape by an arbitrarily chosen parametric family of distributions, we appeal to well-known results from the extreme value theory (EVT) literature. From EVT, we know that the conditional cumulative distribution function (cdf) $G(\varepsilon_t | \mathcal{F}_{t-1})$ of ε_t can under very general conditions be approximated by $G(e_t | \mathcal{F}_{t-1}) = G(\tau | \mathcal{F}_{t-1}) + (1 - G(\tau | \mathcal{F}_{t-1}))P(x_t; \delta_t, \xi_t)$ with $x_t = e_t - \tau$ for sufficiently high thresholds

$\tau \in \mathbb{R}_+$, or more precisely,

$$\begin{aligned} & \limsup_{\tau \rightarrow \infty} \sup_{e_t \geq \tau} |\mathbb{P}[\varepsilon_t \leq e_t + \tau \mid \varepsilon_t > \tau, \mathcal{F}_{t-1}] - P_{\xi_t, \delta_t}(e_t - \tau)| \\ &= \limsup_{\tau \rightarrow \infty} \sup_{e_t \geq \tau} \left| \frac{G(e_t + \tau \mid \mathcal{F}_{t-1}) - G(e_t \mid \mathcal{F}_{t-1})}{1 - G(e_t \mid \mathcal{F}_{t-1})} - P_{\xi_t, \delta_t}(e_t - \tau) \right| = 0, \end{aligned} \quad (2)$$

for parameters $\xi_t = \alpha_t^{-1}$ and δ_t , both possibly depending on τ . Here, $P(x_t; \delta_t, \xi_t)$ denotes the cdf of the Generalized Pareto Distribution (GPD), with cdf and pdf given by

$$P(x_t; \delta_t, \xi_t) = 1 - \left(1 + \xi_t \frac{x_t}{\delta_t}\right)^{-\xi_t^{-1}}, \quad p(x_t; \delta_t, \xi_t) = \delta_t^{-1} \cdot \left(1 + \xi_t \frac{x_t}{\delta_t}\right)^{-\xi_t^{-1}-1}, \quad (3)$$

respectively (see, for example, [McNeil et al., 2010](#)). The quantity $x_t = \varepsilon_t - \tau > 0$ is the so-called peak-over-threshold (POT), or exceedance, of heavy-tailed data ε_t over a pre-determined threshold τ , and $\delta_t > 0$ and $\xi_t > 0$ are the scale and tail shape parameter of the GPD, respectively. Most continuous distributions used in statistics and the actuarial sciences lie in the Maximum Domain of Attraction (MDA) of the GPD (see [McNeil et al., 2010](#), Chapter 7.1), meaning that they allow for the above tail shape approximation. By focusing on the tail area directly using EVT arguments, we avoid having to make more ad-hoc assumptions on the parametric form of the tail.

The result in (2) is a limiting result. In any finite sample, the threshold τ_t has to be set to a specific, finite value, such that the GPD approximation will be inexact and the distribution is in that sense misspecified. This will also be the case in our setting. The score-driven updates that we define later on for ξ_t and δ_t , however, still ensure that the expected Kullback-Leibler divergence between the approximate GPD model and the true, unknown conditional distribution $\mathbb{P}[\varepsilon_t \leq e_t + \tau \mid \varepsilon_t > \tau, \mathcal{F}_{t-1}]$ is improved every time for sufficiently small steps, even if the GPD model is misspecified; see [Blasques et al. \(2015\)](#). The choice of the threshold τ is subject to a well-known bias-efficiency trade-off; see, for instance, [McNeil and Frey \(2000\)](#). In theory, the GPD tail approximation only becomes exact for $\tau \rightarrow +\infty$. A high threshold, however, also implies a smaller number of exceedances $\varepsilon_t > \tau$, and more estimation error for the parameters of the GPD. Common choices for τ from

the literature are the 90%, 95%, and 99% empirical quantiles of ε_t ; see [Chavez-Demoulin et al. \(2014\)](#). We return to the choice, and modeling, of the threshold further below.

A key step in (3) is that we use the conditional probabilities based on the information set \mathcal{F}_{t-1} . As a result, the tail shape parameters become time-varying. To capture this time-variation, we model $(\xi_t, \delta_t)'$ using the score-driven (GAS) dynamics introduced by [Creal et al. \(2013\)](#) and [Harvey \(2013\)](#). In our time series setting, that implies that both δ_t and ξ_t are measurable with respect to \mathcal{F}_{t-1} . We ensure positivity of δ_t and ξ_t by using an (element-wise) exponential link function $(\xi_t, \delta_t)' = \exp(f_t)$ for $f_t = (f_t^\xi, f_t^\delta)' \in \mathbb{R}^2$.² The transition dynamics for f_t are given by so-called GAS(p, q)-dynamics as

$$f_{t+1} = \omega + \sum_{i=0}^{p-1} A_i s_{t-i} + \sum_{j=0}^{q-1} B_j f_{t-j}, \quad (4)$$

$$s_t = \mathcal{S}_t \nabla_t, \quad \nabla_t = \partial \ln p(x_t | \mathcal{F}_{t-1}; f_t, \theta) / \partial f_t,$$

where vector $\omega = (\omega^\xi, \omega^\delta)' = \omega(\theta)$ and matrices $A_i = A_i(\theta)$ and $B_j = B_j(\theta)$ depend on the deterministic parameter vector θ , which needs to be estimated. The scaling matrix \mathcal{S}_t may depend both on θ , f_t , and \mathcal{F}_{t-1} . Effectively, the recursion (4) updates f_t at every time point in time via a scaled steepest ascent step to improve the fit to the GPD. The score of (3) required in (4) is given by

$$\nabla_t = \begin{bmatrix} \xi_t^{-1} \cdot \log(1 + \xi_t \delta_t^{-1} x_t) - (1 + \xi_t^{-1}) \frac{\xi_t x_t}{\delta_t + \xi_t x_t} \\ \frac{x_t - \delta_t}{\delta_t + \xi_t x_t} \end{bmatrix}, \quad (5)$$

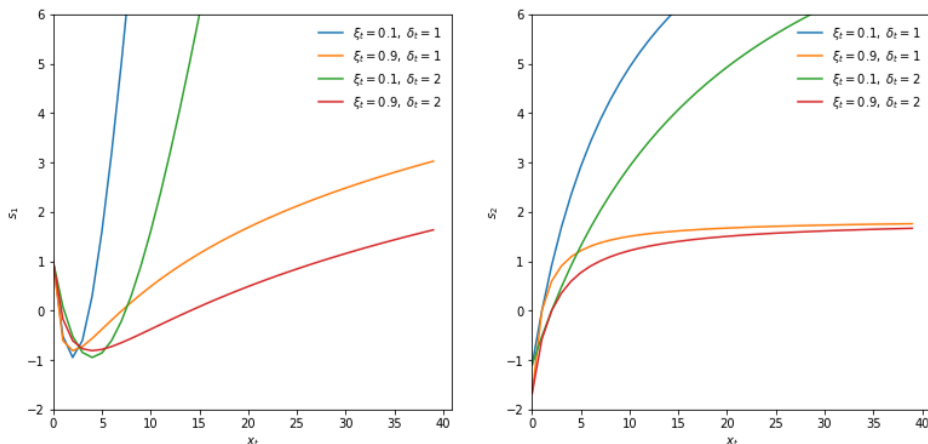
where $\log(\cdot)$ denotes the natural logarithm; see [Appendix A.1](#) for a derivation. We take A_i and B_j as diagonal matrices.

Following [Creal et al. \(2014\)](#) we select the square-root inverse conditional Fisher information of the conditional observation density to scale (5), i.e., $\mathcal{S}_t = L_t'$, with L_t the choleski decomposition of the inverse conditional Fisher information matrix $\mathcal{I}_t = (L_t L_t')^{-1} = \mathbb{E}[\nabla_t \nabla_t' |$

²Given that $\xi_t > 0 \forall t$, (3) is also the cdf and pdf of a Pareto type-II distribution with two time-varying parameters $\alpha_t = \xi_t^{-1}$ and $\sigma_t = \delta_t \xi_t^{-1}$.

Figure 1: News impact curves

The first element (left panel) and second element (right panel) of s_t in (7) is plotted against x_t for different values of ξ_t and δ_t .



$\mathcal{F}_{t-1}; f_t, \theta] = \mathbb{E}[-\partial \nabla_t / \partial f_t' \mid \mathcal{F}_{t-1}; f_t, \theta]$, such that the conditional variance of s_t is equal to the unit matrix. For the GPD, we have

$$L_t = \begin{bmatrix} 1 + \xi_t^{-1} & 0 \\ -1 & \sqrt{1 + 2\xi_t} \end{bmatrix}, \quad (6)$$

see Appendix A.2 for a derivation. Combining terms yields the scaled score as

$$s_t = L_t' \nabla_t = \begin{bmatrix} \xi_t^{-2}(1 + \xi_t) \cdot \log(1 + \xi_t \delta_t^{-1} x_t) + \frac{\delta_t - (\xi_t + 3 + \xi_t^{-1}) \cdot x_t}{\delta_t + \xi_t x_t} \\ \sqrt{1 + 2\xi_t} \frac{x_t - \delta_t}{\delta_t + \xi_t x_t} \end{bmatrix}. \quad (7)$$

Though the scaled score in (7) seems unstable at first sight for ξ_t near zero, the expression actually has a finite limit equal to $\lim_{\xi_t \downarrow 0} s_{1,t} = 1 - 2\delta_t^{-1}x_t + \frac{1}{2}\delta_t^{-2}x_t^2$.

Figure 1 plots the two elements of (7) as a function of x_t for different values of ξ_t and δ_t . The behavior of the scaled score is intuitive: Large x_t imply that f_t is adjusted upwards. For high realization of x_t the adjustments are greatest when the current tail shape and tail scale are low. The function shapes become increasingly concave as $x \rightarrow \infty$ in line with robust updates of the time-varying parameters. This distinguishes our current set-up sharply from

an approach directly based on quantile functions; see [Patton et al. \(2019\)](#) and [Catania and Luati \(2019\)](#), in particular for risk measures such as ES. In [Patton et al. \(2019\)](#), ES reacts linearly to the VaR exceedance. This can result in noisy or unstable ES estimates. Using the GPD shape as emanating from EVT, [Figure 1](#) shows that ξ_t and δ_t react more modestly to large POT observations. This makes sense, as we expect such ‘outliers’ to occur more often for higher values of ξ_t . For extremely high $\xi_t \geq 1$, the ES even ceases to exist. We also note that small realizations of x_t imply downward adjustments of both elements of f_t , up to the point where x_t becomes very small. In that case f_t^ξ is adjusted upward, as observations near the center of a fat-tailed distribution signal increased peakedness (=leptokurtosis); see also [Lucas and Zhang \(2016\)](#). The score-driven steps in (7) can thus result in more stable and interpretable parameter paths due to the concavity of the news impact curves.

When there is no tail observation, i.e. $x_t = \varepsilon_t - \tau \leq 0$, then the new observation carries no information about ξ_t and δ_t ; see [McNeil et al. \(2010, Chapter 7\)](#). In such cases we set the score to zero, and continue to use (4) to update f_t .³ Long consecutive stretches of zero scores can lead to erratic paths for f_t and thus (ξ_t, δ_t) . In addition, such stretches of zero scores can be problematic for inference on θ ; see [Blasques et al. \(2018\)](#). Both issues can be addressed by taking into account lagged values of the scaled score via the exponentially-weighted moving average specification

$$f_{t+1} = \omega + A\tilde{s}_t + Bf_t, \quad (8)$$

where $\tilde{s}_t = (1 - \lambda)s_t + \lambda\tilde{s}_{t-1}$, $\lambda \in (0, 1)$ is an additional parameter to be estimated, and s_t is given by (7). While s_t is most often zero, \tilde{s}_t is not. Clearly, (4) is a special case of (8) for $\lambda \rightarrow 0$. Specification (8) leads to a GAS(1,2) specification for f_t ,

$$(\mathbf{I}_2 - BL)(1 - \lambda)^{-1}(1 - \lambda L)f_{t+1} = \omega + As_t,$$

where L is the lag operator. To see this, first rewrite (8) to $(\mathbf{I}_2 - BL)f_{t+1} = \omega + A\tilde{s}_t$, and then multiply both sides by $(1 - \lambda L)/(1 - \lambda)$, using $(1 - \lambda L)\tilde{s}_t = (1 - \lambda)s_t$. The smoothing

³If $\omega = 0$, $B = I_2$, and $p = q = 1$ in (4), then a zero score implies that both tail parameters retain their current values. We adopt this specification in [Section 4](#) below.

approach in (8) is similar to the approach in Patton (2006) that uses up to ten lags of the driver (in our case the score) to smooth the dynamics of the time-varying parameter.

The transition equation for f_t can be extended further if additional conditioning variables are available. For example, central bank sovereign bond purchases may help explain the time-variation in the tail shape and tail scale parameters associated with changes in sovereign bond yields; see Section 4. Such additional variables can be taken into account in a straightforward way via the modified transition equation,

$$f_{t+1} = \omega + A\tilde{s}_t + Bf_t + C \cdot z_t, \quad (9)$$

where all explanatory variables are stacked into vector z_t , and C is a conformable matrix of impact coefficients that needs to be estimated.

We consider three different ways to set the relevant thresholds. The thresholds can be either time-invariant (τ) or time-varying (τ_t). The construction of the thresholds can be important in practice because τ_t determines whether an observation lies in the tail, and, if so, what is the magnitude of the exceedance $x_t = \varepsilon_t - \tau_t > 0$. The κ -quantile $Q_{1:T}^\kappa(\{\varepsilon_1, \dots, \varepsilon_T\})$ associated with the full sample is an obvious first candidate, $\kappa \in (0, 1)$. In this case, $\tau = Q_{1:T}^\kappa(\{\varepsilon_1, \dots, \varepsilon_T\})$ is time-invariant. Alternatively, we can compute the quantile recursively up to time t and set $\tau_t = Q_{1:t}^\kappa(\{\varepsilon_1, \dots, \varepsilon_t\})$, such that τ_t is time-varying. Finally, we consider a dynamic specification as suggested by Patton et al. (2019), according to which

$$\tau_{t+1} = \tau_t + a^\tau \cdot (1\{\varepsilon_t > \tau_t\} - (1 - \kappa)), \quad (10)$$

where a^τ is a parameter to be estimated, and $\tau_1 = Q_{1:T}^\kappa$ is used to initialize the process. The recursive specification (10) is a martingale since $\mathbb{E}[1\{\varepsilon_t > \tau_t\} | \mathcal{F}_{t-1}, \theta] = (1 - \kappa)$. The threshold τ_t can now respond to changes in the underlying location, scale, and higher-order moments of ε_t in a straightforward way. This is particularly relevant if the data y_t is not pre-filtered based on an appropriate location-scale model in a first step, for instance if we set $\mu_t = 0$ and $\sigma_t = 1$ in (1), thus modeling the conditional extreme tail shape of y_t directly.

We close this section with a brief comment on parameter interpretability. The tail shape parameter ξ_t can always be interpreted as observation y_t 's contemporaneous inverse tail index α_t^{-1} . By contrast, the estimated scale parameter δ_t need not have a straightforward interpretation in terms of y_t 's conditional variance. For example, assume that y_t were GPD distributed with time-varying tail shape parameter α_t^{-1} and scale σ_t . We can then show that the derived POT x_t also has an exact GPD-distribution, with the *same* tail shape parameter $\xi_t = \alpha_t^{-1}$, but a *different* scale parameter $\delta_{t,\tau} = \sigma_t + \alpha_t^{-1} \cdot \tau$; see Web Appendix B.1 for details. As a result, $\delta_{t,\tau}$ increases with the threshold, varies positively with the tail shape parameter ξ_t , and, importantly, should not be expected to provide a consistent estimate of σ_t . A similar result can be derived if the time series data y_t were Student's t -distributed with scale σ_t and tail index α_t ; see Web Appendix B.2. We return to this issue in our simulation Section 3, where we consider pseudo-true values of both parameters to benchmark how well the model can estimate these.

2.2 Confidence bands for tail shape and scale

Confidence (or standard error) bands allow us to visualize the impact of estimation uncertainty associated with the maximum likelihood estimate $\hat{\theta}$ on the filtered estimates $\hat{f}_t(\hat{\theta})$, and, by extension, also $(\hat{\xi}_t, \hat{\delta}_t)' = \exp(\hat{f}_t(\hat{\theta}))$. Quantifying the uncertainty about these parameter paths is important, as classical EVT estimators of time-invariant tail shape parameters are already typically associated with sizeable standard errors; see e.g. Hill (1975) and Huisman et al. (2001). Our confidence bands are based on the variance of \hat{f}_t , which we denote $V_t = \text{Var}(\hat{f}_t)$. There exist two possible ways to construct these bands. Delta-method-based bands can be devised using a linear approximation of the non-linear transition function for f_t , thus extending Blasques et al. (2016, Section 3.2) to the case of multiple lags. We provide the equations in Web Appendix C. In our empirical application below, however, the linear approximations are typically insufficient to capture the uncertainty in the highly non-linear dynamics for some countries. As a result, delta-method-based bands can become unstable. Therefore, we instead use simulation-based bands as in Blasques et al. (2016, Section 3.3).

Simulation-based confidence bands build on the asymptotic normality of $\hat{\theta}$. In particular,

we draw S parameter values $\hat{\theta}^s$, $s = 1, \dots, S$ from the distribution $N(\hat{\theta}, \hat{W})$, where \hat{W} is the estimated covariance matrix of $\hat{\theta}$, e.g., a sandwich covariance matrix estimator. If the finite-sample distribution of $\hat{\theta}$ were known, that could be used instead. For each draw $\hat{\theta}^s$ we now run the filter for f_t from $t = 1$ to $t = T$, thus obtaining S paths \hat{f}_t^s , for $s = 1, \dots, S$ and $t = 1, \dots, T$. These paths account automatically for all non-linearities in the dynamics for f_t . The simulated bands can now be obtained directly by calculating the appropriate percentiles for each t over the S draws of the paths \hat{f}_t^s for $s = 1, \dots, S$.

2.3 Parameter estimation

Parameter estimates can be obtained in a standard way by numerically maximizing the log-likelihood function. Observation-driven time series models such as (3) – (10) are attractive because the log-likelihood is known in closed form. For a given set of time series observations x_1, \dots, x_T , the vector of unknown parameters θ can be estimated by maximizing the log-likelihood function with respect to θ . The average log-likelihood function is given by

$$\begin{aligned} \mathcal{L}(\theta | \mathcal{F}_T) &= (T^*)^{-1} \sum_{t=1}^T 1\{x_t > 0\} \cdot \ln p(x_t; \delta_t, \xi_t) \\ &= (T^*)^{-1} \sum_{t=1}^T 1\{x_t > 0\} \cdot \left[-\ln(\delta_t) - \left(1 + \frac{1}{\xi_t}\right) \ln \left(1 + \xi_t \frac{x_t}{\delta_t}\right) \right], \end{aligned} \quad (11)$$

where $T^* = \sum_{t=1}^T 1\{x_t > 0\}$ is the number of POT values in the sample. Maximization of (11) can be carried out using a conveniently chosen quasi-Newton optimization method.

Blasques et al. (2020) provide conditions under which the maximum likelihood estimator of θ is consistent and asymptotically normally distributed within the class of correctly-specified score-driven models. They also prove that (quasi-)maximum likelihood estimation of θ can remain consistent (to pseudo-true values) and asymptotically normal even if the score-driven model is misspecified in terms of $\ln p(x_t; f_t)$. This is reassuring since the GPD is never exact for any finite value of $\tau < \infty$. In the presence of misspecification, score updates continue to minimize the local Kullback-Leibler divergence between the true conditional density and the model-implied conditional density, and remain optimal in this sense; see

Blasques et al. (2015). The asymptotic covariance matrix $W = \text{Var}(\hat{\theta})$ then takes its usual sandwich form; see e.g. Davidson and MacKinnon (2004, Ch. 10) and Blasques et al. (2020).

The autoregressive parameter a^τ in (10) cannot be estimated using (11). Another objective function is needed in this case. We suggest using the average quantile regression check function of Koenker (2005, Ch. 3). The optimization problem can be formulated as

$$\begin{aligned} \min_{\{a^\tau\}} T^{-1} \sum_{t=1}^T \rho_\kappa(\epsilon_t - \tau_t) &\iff \min_{\{a^\tau\}} T^{-1} \sum_{t=1}^T (\epsilon_t - \tau_t) (\kappa - 1\{\epsilon_t < \tau_t\}) \\ &\iff \max_{\{a^\tau\}} T^{-1} \sum_{t=1}^T (\epsilon_t - \tau_t) ((1 - \kappa) - 1\{\epsilon_t > \tau_t\}), \end{aligned} \quad (12)$$

where $\rho_\kappa(u_t) = u_t(\kappa - 1\{u_t < 0\})$, and τ_t evolves as in (10). See also Engle and Manganelli (2004) and Catania and Luati (2019) for the use of this objective function in a different dynamic context. In practice, we estimate all thresholds τ_t via (12) before maximizing (11).⁴

2.4 A conditional location–scale–df model

This section introduces a score-driven location–scale–df model that can be used to pre-filter univariate time series data y_t that is arbitrarily fat-tailed, where df denotes the degrees of freedom. The model modifies the setting of Lucas and Zhang (2016) with a Student’s t distribution with time-varying volatility and degrees of freedom parameters to a setting that also allows for a time-varying location μ_t parameter and to more extreme tails ($\nu_t < 2$), in which case the volatility no longer exists, but a time varying scale parameter $\sigma_t > 0$ does exist. Since all parameters are time-varying, using this model minimizes the risk of mistaking time-variation in the center of the distribution for time-variation in the tail, and vice versa. The restriction $\nu_t > 0$ aligns closely with the assumption $\alpha_t > 0$ and $\xi_t > 0$ in Section 2.1.

⁴Numerical gradient-based optimizers, such as e.g. MaxBFGS, may only indicate weak convergence at the optimum of (12). This is due to the piecewise linear objective function. The optimizer at hand may not be suited for such a function, and will end up in a kink. This is not a problem, assuming we are not interested in standard errors for a^τ . Alternatively the interior point algorithm of Koenker and Park (1996) could be used.

For the purposes of pre-filtering, in this section y_t is assumed to be generated by

$$y_t \sim t(y_t; \mu_t, \sigma_t, \nu_t), \quad (13)$$

where $\mu_t = \mathbb{E}[y_t \mid \mathcal{F}_{t-1}]$ if $\nu_t > 1$, and $\sqrt{\nu_t/(\nu_t - 2)} \sigma_t$ is the conditional volatility of y_t if $\nu_t > 2$. All time-varying parameters are modeled in a score-driven way as

$$\mu_{t+1} = \omega^\mu + a^\mu s_t^\mu + b^\mu \mu_t + c^\mu z_t + d^\mu y_t, \quad (14)$$

$$\ln \sigma_{t+1} = \omega^\sigma + a^\sigma s_t^\sigma + b^\sigma \ln \sigma_t + c^\sigma z_t + d^\sigma 1\{y_t > \mu_t\} s_t^{\text{Lev}}, \quad (15)$$

$$\nu_{t+1} = \omega^\nu + a^\nu s_t^\nu + b^\nu \nu_t + c^\nu z_t, \quad (16)$$

where $\omega^{(\cdot)}$, $a^{(\cdot)}$, $b^{(\cdot)}$, $c^{(\cdot)}$, and $d^{(\cdot)}$ are scalar parameters to be estimated, and z_t is a vector of additional conditioning variables which may be available. The required scaled scores are

$$s_t^\mu = \frac{(\nu_t + 3)(y_t - \mu_t)}{\nu_t + \sigma_t^{-2}(y_t - \mu_t)^2}, \quad (17)$$

$$s_t^\sigma = \frac{\nu_t + 3}{2\nu_t} \cdot \left(\frac{(\nu_t + 1)(y_t - \mu_t)^2}{\nu_t \sigma_t^2 + (y_t - \mu_t)^2} - 1 \right), \quad (18)$$

$$s_t^\nu = \frac{1}{2} \left[\frac{\nu_t}{4} \gamma'' \left(\frac{\nu_t + 1}{2} \right) - \frac{\nu_t}{4} \gamma'' \left(\frac{\nu_t}{2} \right) + \frac{1}{2} \frac{\nu_t + 5}{(\nu_t + 1)(\nu_t + 3)} \right]^{-1} \left[\frac{1}{\nu_t} + \gamma' \left(\frac{\nu_t}{2} \right) - \gamma' \left(\frac{\nu_t + 1}{2} \right) + \ln \left(1 + \frac{(y_t - \mu_t)^2}{\nu_t \sigma_t^2} \right) - \frac{\nu_t + 1}{\nu_t} \frac{(y_t - \mu_t)^2}{\nu_t \sigma_t^2 + (y_t - \mu_t)^2} \right], \quad (19)$$

where the functions $\gamma'(x)$ and $\gamma''(x)$ are the first and second derivatives of the log-gamma function. We refer to Web Appendix D for a derivation of (17) – (19).

The “leverage” term $d^\sigma \cdot 1\{y_t > \mu_t\} s_t^{\text{Lev}}$ in (15) allows $\ln \sigma_{t+1}$ to be higher (or lower, depending on the sign of d^σ) when y_t is above its location μ_t . The term $s_t^{\text{Lev}} = s_t^\sigma(y_t) - s_t^\sigma(\mu_t)$ is constructed such that the score is continuous at μ_t . Leverage specifications are often found to be valuable in many empirical applications; see e.g. Engle and Patton (2001). The deterministic parameters in (14) – (16) can be estimated by (quasi-)maximum likelihood methods in line with the discussion in Section 2.3.

2.5 Market risk measures

Market risk measurement is a major application of EVT methods in practice; see [Manganeli and Engle \(2004\)](#) and [McNeil et al. \(2010\)](#). We consider the conditional VaR and conditional ES as measures of one-step-ahead market risk. The GPD approximation (2) – (3) yields useful closed-form estimators of the VaR and ES for high upper quantiles $\gamma > G(\tau | \mathcal{F}_{t-1})$; see [McNeil and Frey \(2000\)](#) and [Rocco \(2014\)](#). We can estimate the $1 - \gamma$ tail probability of y_t based on the GPD cdf for x_t , obtaining

$$\begin{aligned} \text{VaR}^\gamma(\epsilon_t | \mathcal{F}_{t-1}, \theta) &= \tau_t + \delta_t \xi_t^{-1} \left[\left(\frac{1 - \gamma}{t^*/t} \right)^{-\xi_t} - 1 \right], \\ \text{VaR}^\gamma(y_t | \mathcal{F}_{t-1}, \theta) &= \mu_t + \sigma_t \text{VaR}^\gamma(\epsilon_t | \mathcal{F}_{t-1}, \theta), \end{aligned} \quad (20)$$

where μ_t and σ_t are defined below (1), and t^* is the number of observations of $x_t > 0$ up to time t , i.e., the number of observations y_s for $s = 1, \dots, t$ for which $y_s > \tau_s$. Put differently, t^*/t is an estimator of the tail probability $\kappa_t = G(\tau_t | \mathcal{F}_{t-1})$.

The conditional ES is the average conditional VaR in the tail across all quantiles γ (see [McNeil et al., 2010](#), Chapter 2), provided $\xi_t < 1$. The closed-form expressions are

$$\begin{aligned} \text{ES}^\gamma(\epsilon_t | \mathcal{F}_{t-1}, \theta) &= \frac{1}{1 - \gamma} \int_\gamma^1 \text{VaR}^{\tilde{\gamma}}(\epsilon_t | \mathcal{F}_{t-1}, \theta) d\tilde{\gamma} \\ &= \frac{\text{VaR}^\gamma(\epsilon_t | \mathcal{F}_{t-1}, \theta)}{1 - \xi_t} + \frac{\delta_t - \xi_t \tau_t}{1 - \xi_t}, \\ \text{ES}^\gamma(y_t | \mathcal{F}_{t-1}, \theta) &= \mu_t + \sigma_t \text{ES}^\gamma(\epsilon_t | \mathcal{F}_{t-1}, \theta); \end{aligned} \quad (21)$$

see Web Appendix E for a derivation of (20) – (21). The $\text{ES}^\gamma(y_t | \cdot)$ is strictly higher than the $\text{VaR}^\gamma(y_t | \cdot)$ at the same confidence level, as it “looks further into the tail.” It can be shown that the ratio $\text{ES}^\gamma(y_t | \cdot) / \text{VaR}^\gamma(y_t | \cdot)$ increases monotonically in ξ_t for $\gamma \rightarrow 1$, indicating that expected losses beyond the VaR become increasingly worse for heavier-tailed (higher ξ_t) distributions. Maximum likelihood estimators of the conditional VaR and conditional ES can be obtained by inserting filtered estimates of μ_t , σ_t , ξ_t and δ_t into (20) and (21).

For later reference, the sensitivity of $\text{VaR}^\gamma(y_t)$ to bond purchases z_{t-1} is given by

$$\frac{d\text{VaR}^\gamma(y_t)}{dz_{t-1}} = \frac{\partial\text{VaR}}{\partial\mu_t} \frac{d\mu_t}{dz_{t-1}} + \frac{\partial\text{VaR}}{\partial\sigma_t} \frac{d\sigma_t}{d\ln\sigma_t} \frac{d\ln\sigma_t}{dz_{t-1}} + \frac{\partial\text{VaR}}{\partial\delta_t} \frac{d\delta_t}{df_t^\delta} \frac{df_t^\delta}{dz_{t-1}} + \frac{\partial\text{VaR}}{\partial\xi_t} \frac{d\xi_t}{df_t^\xi} \frac{df_t^\xi}{dz_{t-1}}.$$

The expression is intuitive: extreme upper quantiles can change if bond purchases z_{t-1} affect the conditional location μ_t , the conditional scale σ_t , the tail scale δ_t , or the tail shape ξ_t .

The derivative is given by

$$\begin{aligned} \frac{d\text{VaR}^\gamma(y_t)}{dz_{t-1}} = & c^\mu + \sigma_t \text{VaR}^\gamma(\epsilon_t) c^\sigma + \sigma_t (\text{VaR}^\gamma(\epsilon_t) - \tau_t) c^\delta \\ & - \sigma_t \left\{ \text{VaR}^\gamma(\epsilon_t) - \tau_t + \delta_t \left(\frac{1-\gamma}{t^*/t} \right)^{-\xi_t} \ln \left(\frac{1-\gamma}{t^*/t} \right) \right\} c^\xi, \end{aligned} \quad (22)$$

where μ_t and σ_t are given by (14) and (15), f_t^ξ and f_t^δ are given by (9) with $C = (c^\delta, c^\xi)'$.

3 Simulation study

This section studies the question whether our score-driven modeling approach can reliably recover the time series variation in tail shape and tail scale in a variety of potentially challenging settings. In addition, we are interested in how to best choose the thresholds τ_t , as well as the accuracy of EVT-based market risk measures when used in combination with our modeling approach.

3.1 Simulation design

Our simulation design considers $D = 2$ different densities (GPD and t), $P = 4$ different parameter paths for tail shape and tail scale, and $H = 3$ different ways to obtain the appropriate thresholds τ_t . This yields $2 \times 4 \times 3 = 24$ simulation experiments. In each experiment, we draw $S = 100$ univariate simulation samples of length $T = 25,000$. We focus on the upper $1 - \kappa = 5\%$ tail. As a result, approximately $25,000 \cdot 0.05 = 1,250$ observations are available in each simulation to compute informative POTs $x_t > 0$. The time series dimension T is chosen to resemble that of the empirical data considered in Section 4.

GPD and t -densities: We first simulate y_t from a GPD distribution with time-varying tail shape α_t^{-1} and tail scale σ_t , $y_t \sim \text{GPD}(\alpha_t^{-1}, \sigma_t)$. We then consider a Student's t distribution with time-varying scale σ_t and degrees of freedom α_t , $y_t \sim t(0, \sigma_t, \alpha_t)$. POT values x_t are obtained as $x_t = y_t - \tau_t$.

Parameter paths: We consider four different paths for the tail shape α_t^{-1} and tail scale σ_t parameters. For both GPD and t densities we consider

- (1) Constant: $\alpha_t^{-1} = 0.5$, $\sigma_t = 1$;
- (2) Sine and constant: $\alpha_t^{-1} = 0.5 + 0.3 \sin(4\pi t/T)$, $\sigma_t = 1$;
- (3) Slow sine and frequent sine: $\alpha_t^{-1} = 0.5 + 0.3 \sin(4\pi t/T)$, $\sigma_t = 1 + 0.5 \sin(16\pi t/T)$;
- (4) Synchronized sines: $\alpha_t^{-1} = 0.5 + 0.3 \sin(4\pi t/T)$, $\sigma_t = 1 + 0.5 \sin(4\pi t/T)$.

Path (1) considers the special case of time-invariant tail shape and scale parameters. Naturally, we would want our dynamic framework to cover constant parameters as a special case. Path (2) allows the tail shape to vary considerably between 0.2 and 0.8, while keeping the scale (volatility) of the data constant. This parameter path corresponds to the empirical practice of working with volatility pre-filtered data. Path (3) stipulates that both parameters vary over time. Finally, Path (4) considers the case of synchronized variation in both parameters. This setting may be particularly challenging for two reasons. First, the tail observations occur most frequently when both tail shape and scale are high, making it potentially difficult to disentangle the two effects. Second, less information about the tail is available when both parameters are low simultaneously.

Different thresholds: We consider three thresholds τ_t . First, we use the true time-varying 95%-quantile based on our knowledge of the true density and of α_t and σ_t . This constitutes an infeasible best benchmark. Second, we construct τ_t as the 95%-quantile of the expanding window of data up to time t , i.e. $\tau_t = Q_{1:t}^{0.95}(\{\varepsilon_1, \dots, \varepsilon_t\})$. Finally, we use the recursive specification (10), with a^τ fixed at 0.25, and initialized at $\tau_1 = Q_{1:T}^{0.95}$.

Evaluation metrics: Our main metric for evaluating model performance is the root mean squared error $\text{RMSE} = \frac{1}{S} \sum_{s=1}^S \sqrt{\frac{1}{T} \sum_{t=1}^T (\hat{\xi}_{st} - \bar{\xi}_{st})^2}$, where $\hat{\xi}_{st}$ is the estimated tail

shape parameter in simulation s , $\bar{\xi}_{st}$ is the corresponding (pseudo-)true tail shape, $s = 1, \dots, S$ denotes the simulation run, and $t = 1, \dots, T$ is the number of observations in each draw. The RMSE for the tail scale parameter δ_t is obtained analogously, $\text{RMSE} = \frac{1}{S} \sum_{s=1}^S \sqrt{\frac{1}{T} \sum_{t=1}^T (\hat{\delta}_{st} - \bar{\delta}_{st})^2}$, where $\bar{\delta}_{st}$ denotes the pseudo-true value of δ_{st} . The pseudo-true values $\bar{\xi}_{st}$ and $\bar{\delta}_{st}$ are obtained by numerically minimizing the Kullback-Leibler divergence between the GPD and the data generating process beyond the true time-varying 95% quantile τ_t . As the true conditional density is known at all times in a simulation setting, these pseudo-true benchmarks are easily computed. We note that particularly the GPD scale parameter $\bar{\delta}_t$ may have very different dynamics from σ_t , as it combines dynamics in α_t and σ_t via the EVT limiting expression in (2).

3.2 Simulation results

Table 1 presents root mean squared error (RMSE) statistics for tail shape $\hat{\xi}_{s,t}$, tail scale $\hat{\delta}_{s,t}$, and Value-at-Risk $\widehat{\text{VaR}}_{s,t}$ estimates. Figures F.1 and F.2 in Web Appendix F.1 compare median estimated parameter paths for $\hat{\xi}_t$, $\hat{\delta}_t$, $\widehat{\text{VaR}}^{0.99}$, and $\widehat{\text{ES}}^{0.99}$ to their (pseudo-)true values. Figure 2 is a representative example of the simulation outcomes when y_t is generated by a Student's t distribution.

We focus on three main findings. First, all models seem to work well in recovering the true underlying ξ_t and δ_t dynamics. The median estimates in Figures F.1 and F.2 tend to be close to their (pseudo-)true values. Particularly the sometimes highly non-linear patterns of δ_t are recovered well. The model also captures well the peaks of ξ_t , so the fattest tails. The model needs some time to recognize that the extreme tail has become more benign, i.e., that ξ_t has gone down. The good fit is corroborated by Table 1. Both estimation methods for τ_t only loose about 10% RMSE for ξ_t and δ_t compared to the use of the true (infeasible) τ_t .

Second, when comparing the recursive estimate $\hat{\tau}_t$ versus the dynamic τ_t^* of Patton et al. (2019) in Table 1, differences are mostly small and insignificant. If there is no time-variation (path (1)), the recursive estimate does slightly better, as expected. The converse is true for δ_t if the true parameters vary over time.

Table 1: Simulation RMSE results

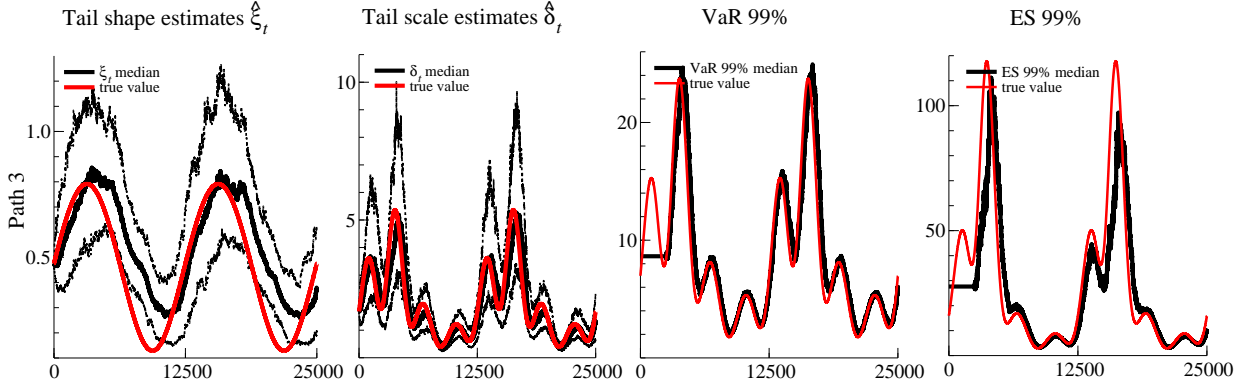
Root mean squared error (RMSE) statistics for two different distributions (GPD and t, in columns) and for four different parameter paths for tail shape ξ_t and tail scale δ_t (paths (1) – (4), in rows). Thresholds τ_t , $\hat{\tau}_t$, and $\hat{\tau}_t^*$ denote *i*) the infeasible true time-varying threshold, *ii*) the empirical quantile associated with an expanding window of observations y_1, \dots, y_t , and *iii*) the estimated conditional quantile using (12) with $a^\tau = 0.25$, respectively. We consider 100 simulations for each DGP, and a time series of 25,000 observations in each simulation. Model performance is measured by the RMSE from the true $\bar{\xi}_t$ and $\bar{\delta}_t$ in each draw. For VaR, model performance is measured in relative terms as RMSE rescaled by the squared VaR_t .

Model	GPD(τ_t) (infeasible)	GPD($\hat{\tau}_t$)	GPD($\hat{\tau}_t^*$)	t(τ_t) (infeasible)	t($\hat{\tau}_t$)	t($\hat{\tau}_t^*$)
RMSE $\hat{\xi}_{s,t}$						
(1)	0.000 (0.000)	0.000 (0.000)	0.000 (0.000)	0.000 (0.000)	0.000 (0.000)	0.000 (0.000)
(2)	0.171 (0.002)	0.177 (0.002)	0.178 (0.002)	0.182 (0.002)	0.188 (0.002)	0.189 (0.002)
(3)	0.182 (0.002)	0.188 (0.002)	0.189 (0.002)	0.190 (0.002)	0.197 (0.002)	0.197 (0.002)
(4)	0.177 (0.002)	0.186 (0.002)	0.183 (0.002)	0.188 (0.002)	0.195 (0.002)	0.192 (0.002)
RMSE $\hat{\delta}_{s,t}$						
(1)	0.005 (0.003)	0.014 (0.006)	0.068 (0.013)	0.005 (0.002)	0.010 (0.004)	0.034 (0.006)
(2)	1.646 (0.034)	1.774 (0.040)	1.753 (0.036)	0.580 (0.013)	0.589 (0.012)	0.588 (0.013)
(3)	2.421 (0.054)	2.913 (0.054)	2.813 (0.049)	0.836 (0.015)	0.960 (0.020)	0.924 (0.017)
(4)	2.608 (0.057)	2.904 (0.059)	2.844 (0.059)	0.925 (0.020)	0.970 (0.020)	0.964 (0.022)
RMSE $\widehat{\text{VaR}}_{s,t}$						
(1)	0.001 (0.001)	0.003 (0.002)	0.016 (0.003)	0.124 (0.001)	0.124 (0.001)	0.149 (0.002)
(2)	0.924 (0.027)	0.987 (0.032)	0.964 (0.031)	0.249 (0.003)	0.243 (0.003)	0.257 (0.003)
(3)	1.063 (0.025)	1.304 (0.041)	1.209 (0.033)	0.322 (0.004)	0.344 (0.005)	0.349 (0.004)
(4)	1.020 (0.027)	1.120 (0.028)	1.083 (0.028)	0.302 (0.003)	0.297 (0.003)	0.319 (0.003)

Third, Figure 2 as well as Figures F.1 and F.2 in Web Appendix F.1 corroborate that our EVT-based market risk measures, such as VaR and ES at a high confidence level $\gamma = 0.99$, tend to be estimated sufficiently accurately when used in combination with our modeling approach. The low and high frequency dynamics of the VaR and ES are both captured well. There only appears some under-estimation of the ES at its very peak where tails are extremely fat. Overall, we conclude that the model captures well the dynamics of the

Figure 2: Simulation results: a representative example

Time series data is here generated as $y_t \sim t(0, \sigma_t, \alpha_t)$, where $\alpha_t^{-1} = 0.5 + 0.3 \sin(4\pi t/T)$ and $\sigma_t = 1 + 0.5 \sin(16\pi t/T)$. This is Path 3 in Section 3.1. Pseudo-true parameter values are reported in solid red. The four panels report estimates of ξ_t , δ_t , VaR_t , and ES_t , respectively. Median filtered values are plotted in solid black. The first two panels also indicate the lower 5% and upper 95% quantiles of the estimates (black dots). The time-varying threshold $\hat{\tau}_t$ is estimated based on the recursive specification (10) in conjunction with the objective function (12).



tails, even if the model does not coincide with the data generating process and is therefore misspecified.

4 The tail impact of Eurosystem asset purchases

4.1 Data

4.1.1 High-frequency data on bond yields

We obtain high-frequency data on changes in euro area sovereign bond yields from Thomson Reuters/Datastream, focusing on Spanish (EN), Greek (GR), Irish (IE), Italian (IT), and Portuguese (PT) five-year sovereign benchmark bonds. These market segments were among the most affected by the euro area debt crisis; see e.g. ECB (2014). SMP bond purchases undertaken during the debt crisis predominantly targeted the two- to ten-year maturity bracket, with the five-year maturity approximately in the middle of that spectrum. We focus on the impact on five-year benchmark bonds for this reason. We model the midpoint between ask and bid prices. Bond prices are expressed in yields-to-maturity and are obtained from continuous dealer quotes.

Our sample ranges from 04 January 2010 to 31 December 2012, covering the most intense phase of the euro area sovereign debt crisis. The bond yields are sampled at the 15-minute frequency between 8AM and 6PM. Following [Ghysels et al. \(2017\)](#) we do not consider overnight changes in yield, such that the first 15-minute interval covers 8AM to 8:15AM. This yields 40 intra-daily observations per trading day. This yields 40 intra-daily observations per day, with $T \approx 3 \times 260 \times 40 \approx 31,000$ observations per country.

The Greek data are an exception. Greek bonds experienced a credit event on 09 March 2012. In January and February 2012 the five-year benchmark bond continued trading, infrequently and at low prices, until approximately one week before the credit event. Our Greek data sample ends on 02 March 2012 for this reason. We include the Greek pre-default data as a truly extreme case, allowing us to “stress-test” our EVT estimation methodology.

Figure [F.3](#) in the Web Appendix [F.2](#) plots the yield-to-maturity of our five benchmark bond yields in levels and in first differences. All five yields exhibited large and sudden moves, leading to volatility clustering and extreme realizations of yield changes during the euro area sovereign debt crisis.

Table [2](#) provides summary statistics for changes in our five benchmark bond yields sampled at the 15-minute frequency. All time series have significant non-Gaussian features under standard tests and significance levels. In particular, we note the non-zero skewness and large values of kurtosis for almost all time series in the sample. Yield changes are covariance stationary according to standard unit root (ADF) tests. Most yield changes are below one bps in absolute value. This suggests that the data are not only heavy-tailed, but also extremely peaked around zero in the center. The pronounced non-Gaussian data features strongly suggest a non-Gaussian empirical framework for modeling conditional location, dispersion, and higher-order moments.

4.1.2 High-frequency data on Eurosystem bond purchases

We study the impact of SMP bond purchases between 2010 and 2012 for five euro area countries: Greece, Ireland, Italy, Portugal, and Spain. At the end of our sample, the Eurosystem held €99.0 bn in Italian sovereign bonds, €30.8 bn in Greek debt, €43.7 bn in Spanish debt,

Table 2: Data descriptive statistics

Summary statistics for changes in five-year sovereign benchmark bond yields measured in percentage points. Columns labeled EN, GR, IE, IT, and PT refer to Spanish, Greek, Irish, Italian, and Portuguese five-year benchmark bond yields. The sample ranges from 04 January 2010 to 28 December 2012. The Greek sample ends on 02 March 2012. Reported p-values for skewness and kurtosis refer to [D'Agostino et al. \(1990\)](#)'s test. The last row reports the fraction of yield changes smaller than one basis point in absolute value.

	EN	GR	IE	IT	PT
Median	0.00	0.00	0.00	0.00	0.00
Std. dev.	0.02	0.46	0.06	0.03	0.08
Minimum	-0.74	-20.73	-0.91	-0.39	-1.15
Maximum	0.47	14.77	1.45	0.43	1.20
Skewness	-42.29	-104.76	34.11	14.91	12.40
Skew. p-value	0.00	0.00	0.00	0.00	0.00
Kurtosis	357.94	195.05	301.26	293.40	279.44
Kurt. p-value	0.00	0.00	0.00	0.00	0.00
Fraction $y_t < 1$ bp	81%	77%	81%	81%	77%

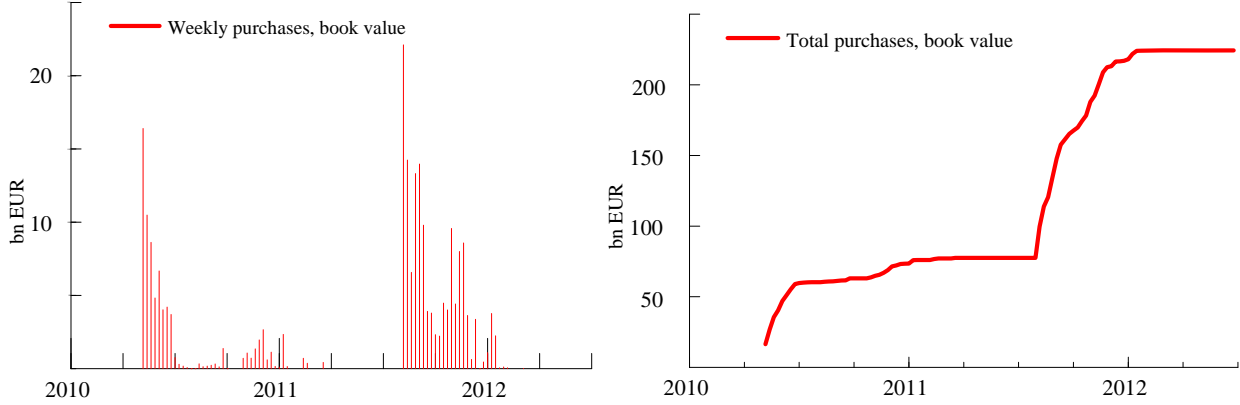
€21.6 bn in Portuguese debt, and €13.6 bn in Irish bonds; see the [ECB \(2013\)](#)'s Annual Report. The SMP's daily cross-country breakdown of the purchase data is still confidential at the time of writing. We use the country-specific data on SMP purchases when studying the impact of the program.

The SMP had the objective of helping to restore the monetary policy transmission mechanism by addressing the malfunctioning of certain government bond markets. The SMP consisted of interventions in the form of outright secondary market purchases. Implicit in the concept of malfunctioning markets is the notion that government bond yields can be unjustifiably high and volatile.

Figure 3 plots weekly total SMP purchases across countries as well as their accumulated book value over time. Approximately €214 billion (bn) of bonds were acquired within the SMP between 2010 and early 2012. The SMP was announced on 10 May 2010 and initially focused on Greek, Irish, and Portuguese debt securities. The program was extended to include Italian and Spanish bonds on 8 August 2011. The SMP was replaced by the Outright Monetary Transactions (OMTs) program on 6 September 2012; see [Cœuré \(2013\)](#). Visibly, the purchase data are unevenly spread over time. Between 10 May 2010 and Spring 2012 there are long periods during which the SMP was open but inactive.

Figure 3: Weekly and total SMP purchase amounts.

The figure plots the book value of settled SMP purchases as of the end of a given week. We report weekly purchases across countries (left panel) as well as the cumulative amounts (right panel). Maturing amounts are excluded.



The SMP purchase data are time-stamped, allowing us to construct time series data z_t of country-specific SMP purchases at the high (15-minute) frequency. The 15-minute frequency is chosen because 15 minutes is the regulatory limit for the recording of trades by the Eurosystem. Observations z_t contain *all* sovereign bond purchases at par (nominal) value between $t - 1$ and t for the respective country, not only purchases of the five-year benchmark bond.

4.2 Location–scale–df model estimates

This section applies our novel location–scale–df model of Section 2.4 to study changes in the yield-to-maturity of five-year sovereign benchmark bonds as discussed in Section 4.1.1. We are particularly interested in each series' location, scale, and degrees of freedom, and how these respond to Eurosystem bond purchases.

We apply the model to the raw data series after removing a (negligible) intra-daily pattern via dummy variable regression. We introduce two simplifications to the general specification. First, preliminary analyses suggest that the location parameters are approximately time-invariant, such that a^μ and b^μ are close to zero. We proceed by imposing this restriction. Note that the specification for the mean still includes $d^\mu \cdot y_{t-1}$ to accommodate a potentially

Table 3: Parameter estimates for the location–scale–df model

Parameter estimates for the univariate location–scale–df model (13). Rows labeled EN, GR, IE, IT, and PT refer to Spanish, Greek, Irish, Italian, and Portuguese five-year benchmark bond yields. The estimation sample ranges from 04 January 2010 to 28 December 2012 for all countries except Greece. Standard error estimates are in round brackets and are taken from a sandwich covariance matrix. P-values are provided in square brackets.

	EN	GR	IE	IT	PT
ω^μ	0.013 (0.007) [0.046]	-0.038 (0.024) [0.108]	0.003 (0.005) [0.641]	-0.003 (0.007) [0.618]	-0.016 (0.006) [0.004]
c^μ (SMP)	-2.623 (0.941) [0.005]	-2.856 (2.483) [0.250]	0.017 (1.594) [0.992]	-1.479 (0.552) [0.007]	-0.053 (2.068) [0.980]
d^μ (AR1)	-0.039 (0.007) [0.000]	-0.000 (0.000) [0.200]	-0.010 (0.002) [0.000]	-0.029 (0.010) [0.004]	-0.004 (0.001) [0.003]
a^σ	0.107 (0.015) [0.000]	0.141 (0.011) [0.000]	0.135 (0.012) [0.000]	0.124 (0.013) [0.000]	0.089 (0.011) [0.000]
c^σ (SMP)	-0.126 (0.089) [0.158]	-0.055 (0.115) [0.635]	-0.461 (0.324) [0.155]	-0.049 (0.050) [0.325]	-0.441 (0.228) [0.053]
d^σ (LEV)	0.004 (0.001) [0.006]	-0.004 (0.001) [0.001]	-0.000 (0.001) [0.885]	0.005 (0.002) [0.002]	-0.000 (0.001) [0.641]
a^ν	0.004 (0.001) [0.000]	0.018 (0.002) [0.000]	0.007 (0.001) [0.000]	0.006 (0.001) [0.000]	0.008 (0.001) [0.000]
c^ν (SMP)	0.031 (0.014) [0.033]	0.042 (0.027) [0.122]	0.022 (0.035) [0.530]	0.013 (0.007) [0.052]	0.000 (0.028) [0.993]
loglik	-56226.2	-68788.4	-68584.7	-56218.6	-78164.0
AIC	112468.4	137592.9	137185.4	112453.2	156343.9
BIC	112534.9	137656.8	137252.0	112519.8	156410.6

negative serial correlation at the 15-minute frequency; see e.g. [Roll \(1984\)](#). Second, we find that the persistence (b^σ and b^ν) in volatility and degrees of freedom parameters is very high. We therefore set $\omega^\sigma = \omega^\nu = 0$ and $b^\sigma = b^\nu = 1$, thus adopting the EWMA restricted score dynamics of [Lucas and Zhang \(2016\)](#) for the scale and df parameters. A comparison of model selection criteria (AIC, BIC) across model specifications confirms these choices. With these simplifications in place, [Table 3](#) now presents the parameter estimates.

We focus on three findings in [Table 3](#). First, SMP bond purchases tended to lower the conditional location of future bond yields for most countries. The estimate of c^μ is negative

for four out of five countries, and is statistically significantly negative for two of them. The estimated impacts for the two largest SMP countries, Italy and Spain, are -1.5 bps and -2.6 bps per €1 bn of purchases, respectively. The highest impact per €1 bn is observed for Greek bonds, at -2.9 bps per €1 bn of purchases. Greek bonds were the most illiquid at the time. The estimates of c^μ for IE and PT are smaller in magnitude and not significant.⁵ Since the yields are modeled in first differences and $a^\mu = b^\mu = 0$, these impacts are associated with long-lasting (permanent) changes in yield *levels*. Overall, our c^μ estimates are in line with those obtained by [Eser and Schwaab \(2016\)](#) based on daily data and factor modeling techniques, and marginally smaller and less dispersed than those obtained by [Ghysels et al. \(2017\)](#) based on high-frequency data and VAR/GARCH modeling techniques.

Second, our parameter estimates for c^σ suggest a reduction in scale (volatility) following SMP bond purchases. The point estimates are all negative, although none are statistically significant at a 5% confidence level. Sizeable standard error estimates for c^σ are intuitive because the SMP intervention data is scarce even at the 15-minute frequency and the log-scale is subject to pronounced time series variation.

Third, the point estimates of c^ν are all positive, and statistically significant in one case (EN, with IT a borderline case). As a result, the time-varying degrees of freedom ν_t tend to increase following SMP bond purchases, suggesting an increasingly “Gaussian” tail shape when the central bank is active as a buyer-of-last-resort. Taken together, the estimates of $c^\mu < 0$, $c^\sigma < 0$, and $c^\nu > 0$ suggest an overall beneficial, market-stabilizing impact of the bond purchases on sovereign bond yields.⁶

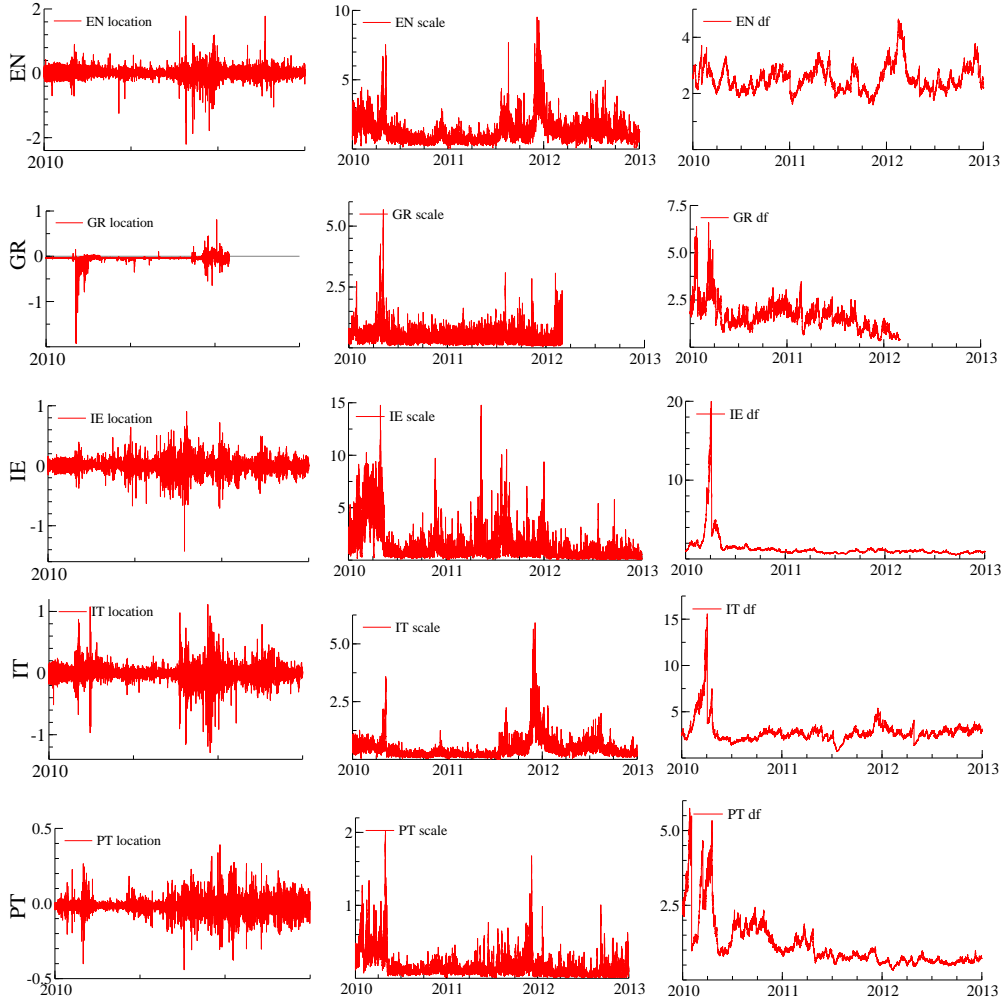
Figure 4.2 plots all time-varying parameters μ_t , σ_t , and ν_t . The conditional location parameters μ_t (left column) tend to be small and rarely exceed one bp in absolute value. The

⁵If SMP purchases were more likely to occur following an increase in yields, then the impact estimates of Table 3 would constitute a lower bound to (the absolute value of) the true impact. This endogeneity is unlikely to be pronounced at the intra-daily frequency because the daily purchase volumes were predetermined before markets opened, constraining the latitude of central bank portfolio managers; see [Eser and Schwaab \(2016, Section 3.3\)](#) for a discussion.

⁶The remaining parameter estimates in Table 3 can be interpreted as follows. The autoregressive coefficients d^μ associated with lagged y_{t-1} are all negative. The implied negative autocorrelation is in line with severely illiquid markets for all five sovereign bonds during our sample; see [Roll \(1984\)](#). The intercept terms ω^μ are small and statistically different from zero only in two out of five cases (for EN and PT). The leverage terms d^σ are positive and statistically significant for EN and IT. In these cases an increase in yield has a greater influence on future log-scale than a decrease.

Figure 4: Filtered location, scale, and degrees of freedom parameters

Filtered location (first column), scale (second column) and degrees of freedom (third column) parameters associated with the location–scale–df model introduced in Section 2.4. Rows labeled EN, GR, IE, IT, and PT refer to Spanish, Greek, Irish, Italian, and Portuguese five-year benchmark bond yields. Greek bonds discontinued trading after 02 March 2012, and experienced a credit event on 09 March 2012.



observed time-variation is due to the inclusion of the lagged term y_{t-1} and bond purchases z_{t-1} . High values for the conditional scale σ_t (middle column) are visible for Greece, Ireland and Portugal in 2010, and for Spain and Italy in late 2011. The conditional df parameters ν_t (right column) suggest that the conditional distribution is profoundly heavy-tailed, even after allowing for time-variation in the location and scale parameters. The df parameter associated with the Greek data declines almost monotonically until the credit event in March 2012.⁷

⁷Quintos et al. (2001) and Lin and Kao (2018) propose Markov-Switching models for the tail index. The

Table 4: Parameter estimates

Parameter estimates for the extended (with SMP purchases z_t) tail shape model. Columns labeled EN, GR, IE, IT, and PT refer to Spanish, Greek, Irish, Italian, and Portuguese five-year benchmark bond yields. The estimation sample ranges from 04 January 2010 to 28 December 2012 for all countries except Greece. Standard error estimates are in round brackets and are constructed from a sandwich covariance matrix. P-values are in square brackets.

	EN	GR	IE	IT	PT
a^ξ	0.006 (0.006) [0.291]	0.032 (0.006) [0.000]	0.021 (0.007) [0.005]	0.055 (0.012) [0.000]	0.026 (0.011) [0.023]
a^δ	0.027 (0.007) [0.000]	0.144 (0.026) [0.000]	0.078 (0.014) [0.000]	0.027 (0.006) [0.000]	0.103 (0.015) [0.000]
c^ξ	0.001 (0.006) [0.847]	0.005 (0.014) [0.705]	0.033 (0.045) [0.467]	-0.009 (0.010) [0.376]	-0.033 (0.029) [0.258]
c^δ	-0.013 (0.014) [0.344]	-0.031 (0.034) [0.362]	0.060 (0.077) [0.433]	-0.011 (0.005) [0.036]	0.107 (0.083) [0.196]
a^τ	0.010	0.312	0.143	0.027	0.263
T	30279	21839	30799	30519	30719
T^*	3003	2223	3093	3041	3084
loglik	-102027.1	-152861.1	-226080.5	-103050.5	-306523.8
AIC	204062.1	305730.2	452168.9	206109.0	613055.7
BIC	204095.4	305762.2	452202.3	206142.3	613089.0

The location–scale–df model (13) is not without drawbacks in our empirical setting. First, it makes an explicit distributional assumption that may or may not be appropriate. Second, it implicitly requires the tail impact of SMP purchases to be symmetric in the lower and upper tail. Since the Eurosystem acted only as a buyer-of-last-resort of bonds between 2010–2012, and has not sold any SMP bonds to date, it is not clear why that should be the case. The next section provides a semi-parametric perspective focussed on the extreme upper (“bad”) tail.

4.3 Tail shape and tail scale estimates

This section discusses our time-varying tail shape (ξ_t) and tail scale (δ_t) estimates associated with the extreme upper tail of changes in sovereign bond yields. We focus on results obtained

location–scale–df estimates reported in Figure 4.2 suggest that these may not be appropriate for our data at hand.

from pre-filtered data, where we used the fitted location–scale–df model from Section 4.2 to clean y_t from location and scale effects. Web Appendix G presents the analogous tail shape and scale estimates from raw bond yield data, allowing us to compare the two approaches; see Section 4.4. Our main results are based on POT observations $x_t = (y_t - \hat{\mu}_t)/\hat{\sigma}_t - \hat{\tau}_t$ if $(y_t - \hat{\mu}_t)/\hat{\sigma}_t > \hat{\tau}_t$ and $x_t = \textit{missing}$ otherwise, where $\hat{\mu}_t$ and $\hat{\sigma}_t$ are the location and scale estimates as reported in Figure 4.2, and where $\hat{\tau}_t$ was obtained using the autoregressive specification (10) in conjunction with the objective function (12).

Preliminary analyses suggest that changes in the tail shape and scale parameters are highly persistent for our high-frequency data. We thus set $\omega^\xi = \omega^\delta = 0$ and $b^\xi = b^\delta = 1$ to simplify the model, again adopting the EWMA restricted score dynamics of Lucas and Zhang (2016) for these parameters. We also set the smoothing parameter $\lambda = 0$, see (7), given the absence of mean reversion in $\ln \xi_t$ and $\ln \delta_t$ at the 15-minute frequency.⁸ We allow $C \neq 0$ such that SMP bond purchases z_{t-1} can impact both $\ln \xi_t$ and $\ln \delta_t$ via their impact coefficients c^ξ and c^δ . A comparison of unreported model selection criteria (AIC, BIC) across different model specifications supports these choices.

Table 4 presents tail shape estimates based on pre-filtered data. Parameters a^ξ and a^δ can be interpreted as the standard deviations of the scores driving $\ln \xi_t$ and $\ln \delta_t$, respectively; see the statements above (6). The associated estimates suggest pronounced time series variation in both parameters. The SMP impact parameters c^ξ are estimated negatively in two out of five cases, but are not statistically significant according to their t-values. Estimates of c^δ are negative in three out of five cases, and are significantly negative in one case (IT). As a result, most of the tail impact of SMP purchases appears to have come about through its impact on the center of the distribution (μ_t, σ_t) and not on its tail shape (δ_t, ξ_t) .

Figure 5 plots the corresponding filtered estimates for time-varying tail shape ξ_t and tail scale δ_t . Blue bars indicate the approximate timing of SMP purchases in the respective markets. Time series variation is present and pronounced in both tail shape and tail scale parameters. The heaviest tail is estimated for Greek bonds during the weeks preceding the

⁸The smoothing parameter λ is hard to estimate numerically given the absence of mean reversion in our high-frequency data. Fixing it to reasonable alternative values has little effect on our empirical findings.

Figure 5: Filtered tail shape and tail scale estimates

Filtered ξ_t and δ_t estimates for Spanish (EN), Greek (GR), Irish (IE), Italian (IT), and Portuguese (PT) five-year sovereign benchmark bond yields between 2010 and 2012. The sample for Greek bonds is shorter as these bonds discontinued trading on 02 March 2012 and experienced a credit event on 09 March 2012. Standard error bands are simulated at a 95% confidence level. Blue bars indicate the approximate timing of SMP purchases in the respective markets. The SMP amounts are first aggregated over all five SMP countries, then smoothed using a centered one-week moving average. The resulting common time series is reported in the respective panel if the SMP was active for the respective market segment at the time; see Section 4.1.2 for the respective announcement days. The scaling of the purchase amounts is omitted and differs between left and right panels only for visibility.

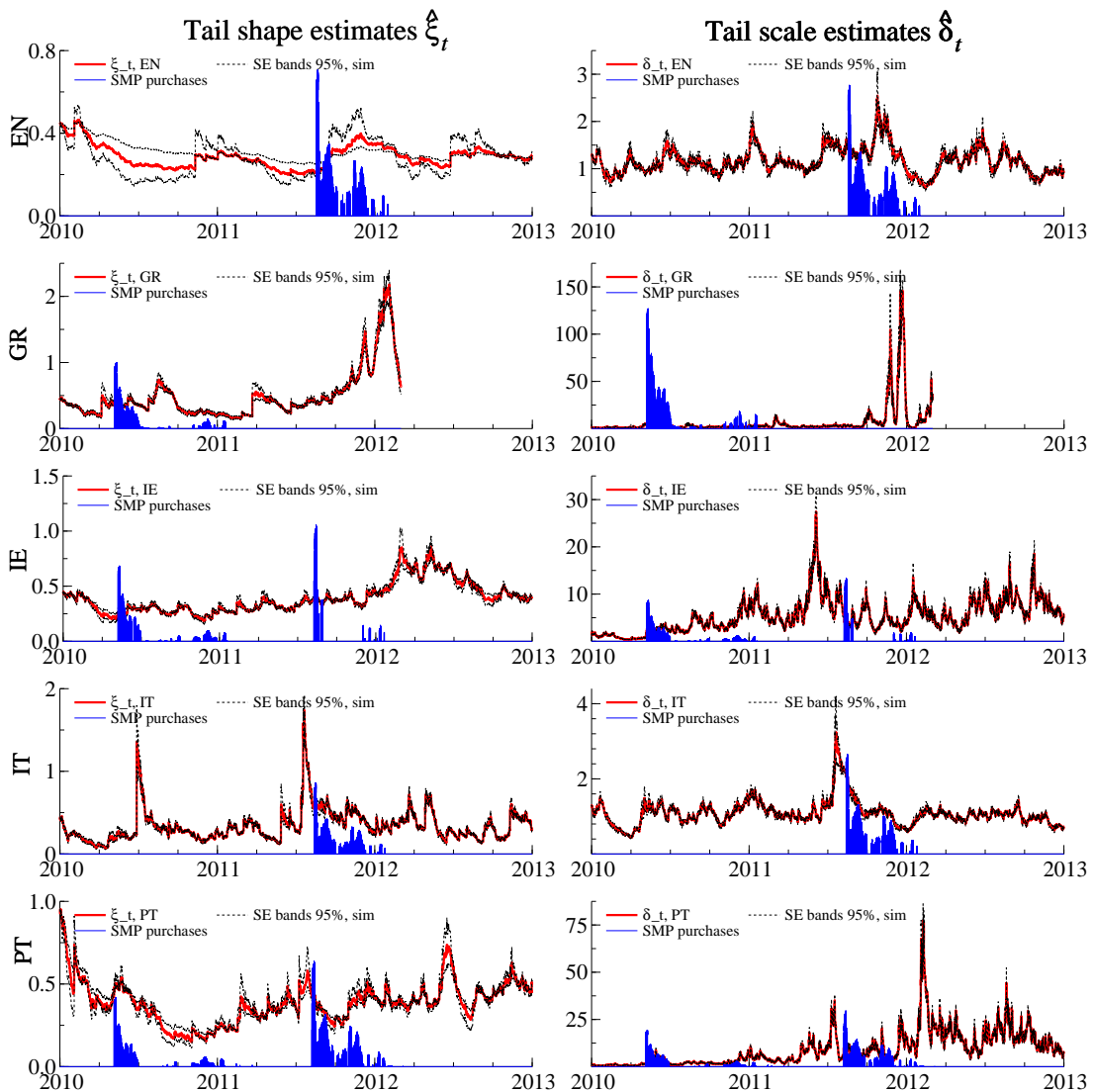


Table 5: Impact of €1 bn of SMP purchases on 97.5% VaR and 99.5% VaR

The table reports the impact of €1 bn of SMP bond purchases on the 97.5% and 99.5% VaR. The total impact is estimated as $(1/\sum_t^T z_t) \sum_t^T (d\text{VaR}^\gamma(y_t)/dz_{t-1}) z_{t-1}$, where $d\text{VaR}^\gamma(y_t)/dz_{t-1}$ is given by (22). The total impact is decomposed into the impact on the conditional location μ_t , scale σ_t , tail scale δ_t , and tail shape ξ_t by setting the non-active summands in (22) to zero. Columns labeled EN, GR, IE, IT, and PT refer to Spanish, Greek, Irish, Italian, and Portuguese five-year benchmark bond yields.

97.5% VaR					
	EN	GR	IE	IT	PT
μ_t	-2.623	-2.856	0.017	-1.479	-0.053
σ_t	-1.155	-2.439	-6.570	-0.537	-8.006
δ_t	-0.068	-0.702	0.587	-0.042	1.216
ξ_t	0.001	0.037	0.068	-0.013	-0.040
Total	-3.845	-5.961	-5.899	-2.071	-6.883
99.5% VaR					
	EN	GR	IE	IT	PT
μ_t	-2.623	-2.856	0.017	-1.479	-0.053
σ_t	-2.302	-5.361	-14.604	-1.163	-18.578
δ_t	-0.190	-2.120	1.638	-0.131	3.556
ξ_t	0.009	0.260	0.443	-0.096	-0.278
Total	-5.106	-10.077	-12.507	-2.870	-15.352

credit event on 09 March 2012. The tail shape parameter can be above one, suggesting that no conditional mean, variance, and ES exist at such times. The other estimates for ξ_t typically vary between zero and one. Estimates above one can occur but are temporary and rare. Time-variation in δ_t is pronounced as well.

The tail shape and scale parameters of Figure 5 are difficult to interpret in economic (or probabilistic) terms when considered in isolation. Table 5 therefore addresses the relevant economic question how market risk measures responded on average to a €1 bn bond purchase intervention. The total impact is decomposed into the impact on the conditional location, scale, tail scale, and tail shape by setting the non-active summands in (22) to zero. The estimates corroborate that most of the SMP's effect on extreme market risk came from its impact on location and scale, and thus from its impact on the center of the distribution. We estimate that the 97.5% VaR was reduced by 3.8, 6.0, 5.9, 2.1, and 6.9 bps per €1 bn Eurosystem intervention in Spanish, Greek, Irish, Italian, and Portuguese five-year bench-

mark bonds, respectively. The impact grows with the extremeness of the VaR. The 99.5% VaR estimate is reduced, respectively, by 5.1, 10.1, 12.5, 2.9, and 15.4 bps per €1 bn of Eurosystem purchases in the above bonds. These are economically meaningful reductions in market risk. Lower market risks likely helped market makers and dealer banks at the time to remain in the market and to continue to supply liquidity to turbulent bond market segments; see e.g. [Pelizzon et al. \(2013, 2016\)](#). High market risks can force dealer banks to retreat, in particular when their own VaR constraints are binding; see [Vayanos and Vila \(2009\)](#) and [Adrian and Shin \(2014\)](#). In turn, malfunctioning sovereign bond markets can impair a balanced transmission of the common monetary policy stance to all parts of the euro area. Table 5 also shows that these improvements were obtained without worsening the tail parameters. If anything, additional beneficial secondary effects came about via the SMP's effect on tail shape and tail scale parameters for large economies such as Spain and Italy.⁹

4.4 Tail shape and tail scale estimates from raw data

We conclude our empirical study with a discussion of tail shape and tail scale estimates from raw (un-prefiltered) data y_t . The dynamic tail shape and tail scale model of Section 2 could be robust to omitted variation in the center of the distribution $g(y_t | \mathcal{F}_{t-1})$. This is because of two effects. First, the autoregressive specification of τ_t via (10) implies that τ_t can adjust to time variation in the center of the distribution. The resulting exceedances $\tilde{x}_t = y_t - \tilde{\tau}_t$ from unfiltered data can therefore in practice still be close to the exceedances $x_t = (y_t - \mu_t)/\sigma_t - \tau_t$ from pre-filtered data. Second, the dynamic specification of δ_t via (7) implies that the tail scale could mop up omitted time-variation in σ_t , leaving ξ_t free to fit the time-variation in tail shape.

Web Appendix G discusses our tail shape and tail scale estimates obtained from POTs $\tilde{x}_t = y_t - \tilde{\tau}_t$, along with the model's deterministic parameters. The estimates of c^δ , the SMP impact on tail scale, are now negative in all five cases, and are statistically significantly

⁹Additional, beneficial SMP announcement effects are not taken into account in Table 5. This is because both the 09 May 2010 and 08 August 2011 SMP announcements occurred when markets were closed, and are therefore not part of our sample. The VaR impact estimates are conservative in this sense.

negative at a 5% confidence level in two cases. This is intuitive, as δ_t now not only captures dispersion in the tail, but to some extent also in the center. The point estimates of c^ξ remain statistically insignificant. The estimates $\hat{\xi}_t$ and $\hat{\delta}_t$ from un-prefiltered data are more volatile, and visibly different from the estimates from pre-filtered data as reported in Figure 5. This suggests that the score-driven updates of τ_t and δ_t do not fully absorb all variation in μ_t and σ_t for our data at hand. We therefore prefer the estimates based on appropriately prefiltered data.

5 Conclusion

We introduced a semi-parametric modeling framework to study time variation in tail parameters for long univariate time series. To this end we modeled the time variation in the shape and scale parameters of the Generalized Pareto Distribution, which approximates the tail of most heavy-tailed densities used in econometrics and the actuarial sciences. We discussed the handling of non-tail time series observations, inference on deterministic and time-varying parameters, and how to relate tail variation to observed covariates if such variables are available. The model therefore complements and extends recent work based on different methodologies, such as the non-parametric approach to tail index variation of [de Haan and Zhou \(2020\)](#), the time-varying quantile (and ES) approaches of [Patton et al. \(2019\)](#) and [Catania and Luati \(2019\)](#), and the parametric modeling approach of [Massacci \(2017\)](#). We applied the model to study the impact of bond purchases within the Eurosystem’s SMP between 2010 and 2012 on the extreme upper tail of sovereign bond yield changes measured at a high frequency, concluding that the program had a beneficial impact on extreme tail quantiles, leaning against the risk of extremely adverse market outcomes while active. This beneficial impact is mostly explained by moving the center of the predicative distribution to the left and narrowing it, rather than via an impact on tail shape or tail scale parameters.

Evidently, our model for time-varying tail parameters is focussed on capturing marginal features. In many applications it may also be of interest to study the time-varying nature of joint extremes; see e.g. [Castro-Camilo et al. \(2018\)](#), [Escobar-Bach et al. \(2018\)](#), and

Mhalla et al. (2019). In terms of the current application, one could wonder, for example, if the extreme bond yield changes for Portuguese and Greek sovereign bonds, say, were more dependent at certain points in time. We leave such research for future work; but see also Lucas et al. (2014) and Patton and Oh (2018) in this regard.

References

- Adrian, T. and H. S. Shin (2014). Procyclical leverage and Value-at-Risk. *Review of Financial Studies* 27(2), 373–403.
- Blasques, F., P. Gorgi, and S. J. Koopman (2018). Missing observations in observation-driven time series models. *Tinbergen Institute Discussion Paper 2018-013/III*, 1–39.
- Blasques, F., S. J. Koopman, K. Lasak, and A. Lucas (2016). In-sample confidence bands and out-of-sample forecast bands for time-varying parameters in observation-driven models. *International Journal of Forecasting* 32, 875–887.
- Blasques, F., S. J. Koopman, and A. Lucas (2015). Information theoretic optimality of observation driven time series models for continuous responses. *Biometrika* 102(2), 325–343.
- Blasques, F., S. J. Koopman, and A. Lucas (2020). Maximum likelihood estimation for score-driven models. *Tinbergen Institute discussion papers 2014-029/III, update July 2020*, 1–54.
- Castro-Camilo, D., M. de Carvalho, and J. Wadsworth (2018). Time-varying extreme value dependence with application to leading European stock markets. *Annals of Applied Statistics* 12(1), 283–309.
- Catania, L. and A. Luati (2019). Semiparametric modeling of multiple quantiles. *Available at SSRN 3494995*.
- Chavez-Demoulin, V., P. Embrechts, and S. Sardy (2014). Extreme-quantile tracking for financial time series. *Journal of Econometrics* 181(1), 44–52.
- Cœuré, B. (2013). Outright Monetary Transactions, one year on. Speech at the conference “The ECB and its OMT programme,” Berlin, 2 September 2013.

- Coles, S. (2001). *An introduction to statistical modeling of extreme values*. Springer Press, London.
- Cox, D. R. (1981). Statistical analysis of time series: some recent developments. *Scandinavian Journal of Statistics* 8, 93–115.
- Creal, D., S. J. Koopman, and A. Lucas (2013). Generalized autoregressive score models with applications. *Journal of Applied Econometrics* 28(5), 777–795.
- Creal, D., B. Schwaab, S. J. Koopman, and A. Lucas (2014). An observation driven mixed measurement dynamic factor model with application to credit risk. *The Review of Economics and Statistics* 96(5), 898–915.
- D’Agostino, R. B., A. Belanger, and R. B. D’Agostino Jr (1990). A suggestion for using powerful and informative tests of normality. *The American Statistician* 44(4), 316–321.
- Davidson, A. C. and R. L. Smith (1990). Models for exceedances over high thresholds. *Journal of the Royal Statistical Association, Series B* 52(3), 393–442.
- Davidson, R. and J. G. MacKinnon (2004). *Econometric theory and methods*. Oxford University press.
- de Haan, L. and C. Zhou (2020). Trends in extreme value indices. *Journal of the American Statistical Association*, forthcoming.
- ECB (2013). European Central Bank Annual Report 2012.
- ECB (2014). The determinants of euro area sovereign bond yield spreads during the crisis. ECB Monthly Bulletin article, May 2014.
- Einmahl, J., L. de Haan, and C. Zhou (2016). Statistics of heteroscedastic extremes. *Journal of the Royal Statistical Society, Series B* 78, 31–51.
- Embrechts, P., C. Klüppelberg, and T. Mikosch (1997). *Modelling extremal events for insurance and finance*. Springer Verlag, Berlin.
- Engle, R. F. and S. Manganelli (2004). CAViaR: Conditional autoregressive value at risk by regression quantiles. *Journal of Business & Economic Statistics* 22(4), 367–381.

- Engle, R. F. and A. J. Patton (2001). What good is a volatility model? *Quantitative Finance* 1(2), 237–245.
- Escobar-Bach, M., Y. Goegebeur, and A. Guillou (2018). Local robust estimation of the Pickands dependence function. *Annals of Statistics* 46(6A), 2806–2843.
- Eser, F. and B. Schwaab (2016). Evaluating the impact of unconventional monetary policy measures: Empirical evidence from the ECB’s Securities Markets Programme. *Journal of Financial Economics* 119(1), 147–167.
- Galbraith, J. W. and S. Zernov (2004). Circuit breakers and the tail index of equity returns. *Journal of Financial Econometrics* 2(1), 109–129.
- Ghysels, E., J. Idier, S. Manganelli, and O. Vergote (2017). A high frequency assessment of the ECB Securities Markets Programme. *Journal of European Economic Association* 15(1), 218–243.
- Harvey, A. C. (2013). *Dynamic models for volatility and heavy tails with applications to financial and economic time series*. Cambridge University Press.
- Hill, B. (1975). A simple general approach to inference about the tail of a distribution. *The Annals of Statistics* 3(5), 1163–1174.
- Hoga, Y. (2017). Testing for changes in (Extreme) VaR. *Econometrics Journal* 20, 23–51.
- Huisman, R., K. Koedijk, C. Kool, and F. Palm (2001). Tail-index estimates in small samples. *Journal of Business & Economic Statistics* 19(1), 208–216.
- Koenker, R. (2005). *Quantile Regression*. Cambridge: Cambridge University Press.
- Koenker, R. and B. J. Park (1996). An interior point algorithm for nonlinear quantile regression. *Journal of Econometrics* 71(1-2), 265–283.
- Lin, C.-H. and T.-C. Kao (2018). Multiple structural changes in the tail behavior: evidence from stock market futures returns. *Nonlinear Analysis: Real World Applications* 9, 1702–1713.
- Lucas, A., B. Schwaab, and X. Zhang (2014). Conditional euro area sovereign default risk. *Journal of Business and Economic Statistics* 32(2), 271–284.

- Lucas, A. and X. Zhang (2016). Score driven exponentially weighted moving average and value-at-risk forecasting. *International Journal of Forecasting* 32, 293–302.
- Manganelli, S. and R. F. Engle (2004). A comparison of value at risk models in finance. In G. Szegö (Ed.), *Risk Measures for the 21st Century*. Wiley Finance.
- Massacci, D. (2017). Tail risk dynamics in stock returns: Links to the macroeconomy and global markets connectedness. *Management Science* 63(9), 112–132.
- McNeil, A. and R. Frey (2000). Estimation of tail-related risk measures for heteroscedastic financial time series: An Extreme Value approach. *Journal of Empirical Finance* 7(3-4), 271–300.
- McNeil, A. J., R. Frey, and P. Embrechts (2010). *Quantitative risk management: Concepts, techniques, and tools*. Princeton University press.
- Mhalla, L., M. de Carvalho, and V. ChavezDemoulin (2019). Regressiontype models for extremal dependence. *Scandinavian Journal of Statistics* 46(4), 1141–1167.
- Patton, A. (2006). Modelling asymmetric exchange rate dependence. *International Economic Review* 47(2), 527–556.
- Patton, A. J. and D. H. Oh (2018). Time-varying systemic risk: evidence from a dynamic copula model of CDS spreads. *Journal of Business & Economic Statistics* 36(2), 181–195.
- Patton, A. J., J. F. Ziegel, and R. Chen (2019). Dynamic semiparametric models for Expected Shortfall (and Value-at-Risk). *Journal of Econometrics* 211(2), 388–413.
- Pelizzon, L., M. Subrahmanyam, D. Tomio, and J. Uno (2013). The microstructure of the European sovereign bond market: A study of the Eurozone crisis. Unpublished working paper, University of Venice, New York University, Copenhagen Business School, and Waseda University.
- Pelizzon, L., M. Subrahmanyam, D. Tomio, and J. Uno (2016). Sovereign credit risk, liquidity, and ECB intervention: Deus Ex Machina? *Journal of Financial Economics* 122(1), 44–52.
- Pooter, M. D., R. F. Martin, and S. Pruitt (2018). The liquidity effects of official bond market intervention. *Journal of Financial and Quantitative Analysis* 53(1), 243–268.

- Quintos, C., Z. Fan, and P. C. Phillips (2001). Structural change tests in tail behaviour and the asian crisis. *The Review of Economic Studies* 68(3), 633–663.
- Rocco, M. (2014). Extreme value theory in finance: A survey. *Journal of Economic Surveys* 28(1), 82–108.
- Roll, R. (1984). A simple implicit measure of the effective bid-ask spread in an efficient market. *The Journal of Finance* 39(4), 1127–1139.
- Vayanos, D. and J.-L. Vila (2009). A preferred habitat model of the term structure of interest rates. NBER Working Paper 15487.
- Wagner, N. (2005). Autoregressive conditional tail behavior and results on government bond yield spreads. *International Review of Financial Analysis* 14(2), 247–261.
- Wang, H. and C.-L. Tsai (2009). Tail Index Regression. *Journal of the American Statistical Association* 104(487), 1233–1240.
- Werner, T. and C. Upper (2004). Time variation in the tail behavior of bund future returns. *Journal of Futures Markets* 24(4), 387–398.

Earlier Working Papers:

For a complete list of Working Papers published by Sveriges Riksbank, see www.riksbank.se

Estimation of an Adaptive Stock Market Model with Heterogeneous Agents <i>by Henrik Amilon</i>	2005:177
Some Further Evidence on Interest-Rate Smoothing: The Role of Measurement Errors in the Output Gap <i>by Mikael Apel and Per Jansson</i>	2005:178
Bayesian Estimation of an Open Economy DSGE Model with Incomplete Pass-Through <i>by Malin Adolfson, Stefan Laséen, Jesper Lindé and Mattias Villani</i>	2005:179
Are Constant Interest Rate Forecasts Modest Interventions? Evidence from an Estimated Open Economy DSGE Model of the Euro Area <i>by Malin Adolfson, Stefan Laséen, Jesper Lindé and Mattias Villani</i>	2005:180
Inference in Vector Autoregressive Models with an Informative Prior on the Steady State <i>by Mattias Villani</i>	2005:181
Bank Mergers, Competition and Liquidity <i>by Elena Carletti, Philipp Hartmann and Giancarlo Spagnolo</i>	2005:182
Testing Near-Rationality using Detailed Survey Data <i>by Michael F. Bryan and Stefan Palmqvist</i>	2005:183
Exploring Interactions between Real Activity and the Financial Stance <i>by Tor Jacobson, Jesper Lindé and Kasper Roszbach</i>	2005:184
Two-Sided Network Effects, Bank Interchange Fees, and the Allocation of Fixed Costs <i>by Mats A. Bergman</i>	2005:185
Trade Deficits in the Baltic States: How Long Will the Party Last? <i>by Rudolfs Bems and Kristian Jönsson</i>	2005:186
Real Exchange Rate and Consumption Fluctuations following Trade Liberalization <i>by Kristian Jönsson</i>	2005:187
Modern Forecasting Models in Action: Improving Macroeconomic Analyses at Central Banks <i>by Malin Adolfson, Michael K. Andersson, Jesper Lindé, Mattias Villani and Anders Vredin</i>	2005:188
Bayesian Inference of General Linear Restrictions on the Cointegration Space <i>by Mattias Villani</i>	2005:189
Forecasting Performance of an Open Economy Dynamic Stochastic General Equilibrium Model <i>by Malin Adolfson, Stefan Laséen, Jesper Lindé and Mattias Villani</i>	2005:190
Forecast Combination and Model Averaging using Predictive Measures <i>by Jana Eklund and Sune Karlsson</i>	2005:191
Swedish Intervention and the Krona Float, 1993-2002 <i>by Owen F. Humpage and Javiera Ragnartz</i>	2006:192
A Simultaneous Model of the Swedish Krona, the US Dollar and the Euro <i>by Hans Lindblad and Peter Sellin</i>	2006:193
Testing Theories of Job Creation: Does Supply Create Its Own Demand? <i>by Mikael Carlsson, Stefan Eriksson and Nils Gottfries</i>	2006:194
Down or Out: Assessing The Welfare Costs of Household Investment Mistakes <i>by Laurent E. Calvet, John Y. Campbell and Paolo Sodini</i>	2006:195
Efficient Bayesian Inference for Multiple Change-Point and Mixture Innovation Models <i>by Paolo Giordani and Robert Kohn</i>	2006:196
Derivation and Estimation of a New Keynesian Phillips Curve in a Small Open Economy <i>by Karolina Holmberg</i>	2006:197
Technology Shocks and the Labour-Input Response: Evidence from Firm-Level Data <i>by Mikael Carlsson and Jon Smedsaas</i>	2006:198
Monetary Policy and Staggered Wage Bargaining when Prices are Sticky <i>by Mikael Carlsson and Andreas Westermark</i>	2006:199
The Swedish External Position and the Krona <i>by Philip R. Lane</i>	2006:200

Price Setting Transactions and the Role of Denominating Currency in FX Markets <i>by Richard Friberg and Fredrik Wilander</i>	2007:201
The geography of asset holdings: Evidence from Sweden <i>by Nicolas Coeurdacier and Philippe Martin</i>	2007:202
Evaluating An Estimated New Keynesian Small Open Economy Model <i>by Malin Adolfson, Stefan Laséen, Jesper Lindé and Mattias Villani</i>	2007:203
The Use of Cash and the Size of the Shadow Economy in Sweden <i>by Gabriela Guibourg and Björn Segendorf</i>	2007:204
Bank supervision Russian style: Evidence of conflicts between micro- and macro-prudential concerns <i>by Sophie Claeys and Koen Schoors</i>	2007:205
Optimal Monetary Policy under Downward Nominal Wage Rigidity <i>by Mikael Carlsson and Andreas Westermark</i>	2007:206
Financial Structure, Managerial Compensation and Monitoring <i>by Vittoria Cerasi and Sonja Daltung</i>	2007:207
Financial Frictions, Investment and Tobin's q <i>by Guido Lorenzoni and Karl Walentin</i>	2007:208
Sticky Information vs Sticky Prices: A Horse Race in a DSGE Framework <i>by Mathias Trabandt</i>	2007:209
Acquisition versus greenfield: The impact of the mode of foreign bank entry on information and bank lending rates <i>by Sophie Claeys and Christa Hainz</i>	2007:210
Nonparametric Regression Density Estimation Using Smoothly Varying Normal Mixtures <i>by Mattias Villani, Robert Kohn and Paolo Giordani</i>	2007:211
The Costs of Paying – Private and Social Costs of Cash and Card <i>by Mats Bergman, Gabriella Guibourg and Björn Segendorf</i>	2007:212
Using a New Open Economy Macroeconomics model to make real nominal exchange rate forecasts <i>by Peter Sellin</i>	2007:213
Introducing Financial Frictions and Unemployment into a Small Open Economy Model <i>by Lawrence J. Christiano, Mathias Trabandt and Karl Walentin</i>	2007:214
Earnings Inequality and the Equity Premium <i>by Karl Walentin</i>	2007:215
Bayesian forecast combination for VAR models <i>by Michael K. Andersson and Sune Karlsson</i>	2007:216
Do Central Banks React to House Prices? <i>by Daria Finocchiaro and Virginia Queijo von Heideken</i>	2007:217
The Riksbank's Forecasting Performance <i>by Michael K. Andersson, Gustav Karlsson and Josef Svensson</i>	2007:218
Macroeconomic Impact on Expected Default Frequency <i>by Per Åsberg and Hovick Shahnazarian</i>	2008:219
Monetary Policy Regimes and the Volatility of Long-Term Interest Rates <i>by Virginia Queijo von Heideken</i>	2008:220
Governing the Governors: A Clinical Study of Central Banks <i>by Lars Frisell, Kasper Roszbach and Giancarlo Spagnolo</i>	2008:221
The Monetary Policy Decision-Making Process and the Term Structure of Interest Rates <i>by Hans Dillén</i>	2008:222
How Important are Financial Frictions in the U S and the Euro Area <i>by Virginia Queijo von Heideken</i>	2008:223
Block Kalman filtering for large-scale DSGE models <i>by Ingvar Strid and Karl Walentin</i>	2008:224
Optimal Monetary Policy in an Operational Medium-Sized DSGE Model <i>by Malin Adolfson, Stefan Laséen, Jesper Lindé and Lars E. O. Svensson</i>	2008:225
Firm Default and Aggregate Fluctuations <i>by Tor Jacobson, Rikard Kindell, Jesper Lindé and Kasper Roszbach</i>	2008:226
Re-Evaluating Swedish Membership in EMU: Evidence from an Estimated Model <i>by Ulf Söderström</i>	2008:227

The Effect of Cash Flow on Investment: An Empirical Test of the Balance Sheet Channel <i>by Ola Melander</i>	2009:228
Expectation Driven Business Cycles with Limited Enforcement <i>by Karl Walentin</i>	2009:229
Effects of Organizational Change on Firm Productivity <i>by Christina Håkanson</i>	2009:230
Evaluating Microfoundations for Aggregate Price Rigidities: Evidence from Matched Firm-Level Data on Product Prices and Unit Labor Cost <i>by Mikael Carlsson and Oskar Nordström Skans</i>	2009:231
Monetary Policy Trade-Offs in an Estimated Open-Economy DSGE Model <i>by Malin Adolfson, Stefan Laséen, Jesper Lindé and Lars E. O. Svensson</i>	2009:232
Flexible Modeling of Conditional Distributions Using Smooth Mixtures of Asymmetric Student T Densities <i>by Feng Li, Mattias Villani and Robert Kohn</i>	2009:233
Forecasting Macroeconomic Time Series with Locally Adaptive Signal Extraction <i>by Paolo Giordani and Mattias Villani</i>	2009:234
Evaluating Monetary Policy <i>by Lars E. O. Svensson</i>	2009:235
Risk Premiums and Macroeconomic Dynamics in a Heterogeneous Agent Model <i>by Ferre De Graeve, Maarten Dossche, Marina Emiris, Henri Sneessens and Raf Wouters</i>	2010:236
Picking the Brains of MPC Members <i>by Mikael Apel, Carl Andreas Claussen and Petra Lennartsdotter</i>	2010:237
Involuntary Unemployment and the Business Cycle <i>by Lawrence J. Christiano, Mathias Trabandt and Karl Walentin</i>	2010:238
Housing collateral and the monetary transmission mechanism <i>by Karl Walentin and Peter Sellin</i>	2010:239
The Discursive Dilemma in Monetary Policy <i>by Carl Andreas Claussen and Øistein Røisland</i>	2010:240
Monetary Regime Change and Business Cycles <i>by Vasco Cúrdia and Daria Finocchiaro</i>	2010:241
Bayesian Inference in Structural Second-Price common Value Auctions <i>by Bertil Wegmann and Mattias Villani</i>	2010:242
Equilibrium asset prices and the wealth distribution with inattentive consumers <i>by Daria Finocchiaro</i>	2010:243
Identifying VARs through Heterogeneity: An Application to Bank Runs <i>by Ferre De Graeve and Alexei Karas</i>	2010:244
Modeling Conditional Densities Using Finite Smooth Mixtures <i>by Feng Li, Mattias Villani and Robert Kohn</i>	2010:245
The Output Gap, the Labor Wedge, and the Dynamic Behavior of Hours <i>by Luca Sala, Ulf Söderström and Antonella Trigari</i>	2010:246
Density-Conditional Forecasts in Dynamic Multivariate Models <i>by Michael K. Andersson, Stefan Palmqvist and Daniel F. Waggoner</i>	2010:247
Anticipated Alternative Policy-Rate Paths in Policy Simulations <i>by Stefan Laséen and Lars E. O. Svensson</i>	2010:248
MOSES: Model of Swedish Economic Studies <i>by Gunnar Bårdsen, Ard den Reijer, Patrik Jonasson and Ragnar Nymoén</i>	2011:249
The Effects of Endogenous Firm Exit on Business Cycle Dynamics and Optimal Fiscal Policy <i>by Lauri Vilmi</i>	2011:250
Parameter Identification in a Estimated New Keynesian Open Economy Model <i>by Malin Adolfson and Jesper Lindé</i>	2011:251
Up for count? Central bank words and financial stress <i>by Marianna Blix Grimaldi</i>	2011:252
Wage Adjustment and Productivity Shocks <i>by Mikael Carlsson, Julián Messina and Oskar Nordström Skans</i>	2011:253

Stylized (Arte) Facts on Sectoral Inflation <i>by Ferre De Graeve and Karl Walentin</i>	2011:254
Hedging Labor Income Risk <i>by Sebastien Betermier, Thomas Jansson, Christine A. Parlour and Johan Walden</i>	2011:255
Taking the Twists into Account: Predicting Firm Bankruptcy Risk with Splines of Financial Ratios <i>by Paolo Giordani, Tor Jacobson, Erik von Schedvin and Mattias Villani</i>	2011:256
Collateralization, Bank Loan Rates and Monitoring: Evidence from a Natural Experiment <i>by Geraldo Cerqueiro, Steven Ongena and Kasper Roszbach</i>	2012:257
On the Non-Exclusivity of Loan Contracts: An Empirical Investigation <i>by Hans Degryse, Vasso Ioannidou and Erik von Schedvin</i>	2012:258
Labor-Market Frictions and Optimal Inflation <i>by Mikael Carlsson and Andreas Westermark</i>	2012:259
Output Gaps and Robust Monetary Policy Rules <i>by Roberto M. Billi</i>	2012:260
The Information Content of Central Bank Minutes <i>by Mikael Apel and Marianna Blix Grimaldi</i>	2012:261
The Cost of Consumer Payments in Sweden <i>by Björn Segendorf and Thomas Jansson</i>	2012:262
Trade Credit and the Propagation of Corporate Failure: An Empirical Analysis <i>by Tor Jacobson and Erik von Schedvin</i>	2012:263
Structural and Cyclical Forces in the Labor Market During the Great Recession: Cross-Country Evidence <i>by Luca Sala, Ulf Söderström and Antonella Trigari</i>	2012:264
Pension Wealth and Household Savings in Europe: Evidence from SHARELIFE <i>by Rob Alessie, Viola Angelini and Peter van Santen</i>	2013:265
Long-Term Relationship Bargaining <i>by Andreas Westermark</i>	2013:266
Using Financial Markets To Estimate the Macro Effects of Monetary Policy: An Impact-Identified FAVAR* <i>by Stefan Pitschner</i>	2013:267
DYNAMIC MIXTURE-OF-EXPERTS MODELS FOR LONGITUDINAL AND DISCRETE-TIME SURVIVAL DATA <i>by Matias Quiroz and Mattias Villani</i>	2013:268
Conditional euro area sovereign default risk <i>by André Lucas, Bernd Schwaab and Xin Zhang</i>	2013:269
Nominal GDP Targeting and the Zero Lower Bound: Should We Abandon Inflation Targeting?*	2013:270
<i>by Roberto M. Billi</i>	
Un-truncating VARs* <i>by Ferre De Graeve and Andreas Westermark</i>	2013:271
Housing Choices and Labor Income Risk <i>by Thomas Jansson</i>	2013:272
Identifying Fiscal Inflation* <i>by Ferre De Graeve and Virginia Queijo von Heideken</i>	2013:273
On the Redistributive Effects of Inflation: an International Perspective* <i>by Paola Boel</i>	2013:274
Business Cycle Implications of Mortgage Spreads* <i>by Karl Walentin</i>	2013:275
Approximate dynamic programming with post-decision states as a solution method for dynamic economic models <i>by Isaiah Hull</i>	2013:276
A detrimental feedback loop: deleveraging and adverse selection <i>by Christoph Bertsch</i>	2013:277
Distortionary Fiscal Policy and Monetary Policy Goals <i>by Klaus Adam and Roberto M. Billi</i>	2013:278
Predicting the Spread of Financial Innovations: An Epidemiological Approach <i>by Isaiah Hull</i>	2013:279
Firm-Level Evidence of Shifts in the Supply of Credit <i>by Karolina Holmberg</i>	2013:280

Lines of Credit and Investment: Firm-Level Evidence of Real Effects of the Financial Crisis <i>by Karolina Holmberg</i>	2013:281
A wake-up call: information contagion and strategic uncertainty <i>by Toni Ahnert and Christoph Bertsch</i>	2013:282
Debt Dynamics and Monetary Policy: A Note <i>by Stefan Laséen and Ingvar Strid</i>	2013:283
Optimal taxation with home production <i>by Conny Olovsson</i>	2014:284
Incompatible European Partners? Cultural Predispositions and Household Financial Behavior <i>by Michael Haliassos, Thomas Jansson and Yigitcan Karabulut</i>	2014:285
How Subprime Borrowers and Mortgage Brokers Shared the Piecial Behavior <i>by Antje Berndt, Burton Hollifield and Patrik Sandås</i>	2014:286
The Macro-Financial Implications of House Price-Indexed Mortgage Contracts <i>by Isaiah Hull</i>	2014:287
Does Trading Anonymously Enhance Liquidity? <i>by Patrick J. Dennis and Patrik Sandås</i>	2014:288
Systematic bailout guarantees and tacit coordination <i>by Christoph Bertsch, Claudio Calcagno and Mark Le Quement</i>	2014:289
Selection Effects in Producer-Price Setting <i>by Mikael Carlsson</i>	2014:290
Dynamic Demand Adjustment and Exchange Rate Volatility <i>by Vesna Corbo</i>	2014:291
Forward Guidance and Long Term Interest Rates: Inspecting the Mechanism <i>by Ferre De Graeve, Pelin Ilbas & Raf Wouters</i>	2014:292
Firm-Level Shocks and Labor Adjustments <i>by Mikael Carlsson, Julián Messina and Oskar Nordström Skans</i>	2014:293
A wake-up call theory of contagion <i>by Toni Ahnert and Christoph Bertsch</i>	2015:294
Risks in macroeconomic fundamentals and excess bond returns predictability <i>by Rafael B. De Rezende</i>	2015:295
The Importance of Reallocation for Productivity Growth: Evidence from European and US Banking <i>by Jaap W.B. Bos and Peter C. van Santen</i>	2015:296
SPEEDING UP MCMC BY EFFICIENT DATA SUBSAMPLING <i>by Matias Quiroz, Mattias Villani and Robert Kohn</i>	2015:297
Amortization Requirements and Household Indebtedness: An Application to Swedish-Style Mortgages <i>by Isaiah Hull</i>	2015:298
Fuel for Economic Growth? <i>by Johan Gars and Conny Olovsson</i>	2015:299
Searching for Information <i>by Jungsuk Han and Francesco Sangiorgi</i>	2015:300
What Broke First? Characterizing Sources of Structural Change Prior to the Great Recession <i>by Isaiah Hull</i>	2015:301
Price Level Targeting and Risk Management <i>by Roberto Billi</i>	2015:302
Central bank policy paths and market forward rates: A simple model <i>by Ferre De Graeve and Jens Iversen</i>	2015:303
Jump-Starting the Euro Area Recovery: Would a Rise in Core Fiscal Spending Help the Periphery? <i>by Olivier Blanchard, Christopher J. Erceg and Jesper Lindé</i>	2015:304
Bringing Financial Stability into Monetary Policy* <i>by Eric M. Leeper and James M. Nason</i>	2015:305
SCALABLE MCMC FOR LARGE DATA PROBLEMS USING DATA SUBSAMPLING AND THE DIFFERENCE ESTIMATOR <i>by MATIAS QUIROZ, MATTIAS VILLANI AND ROBERT KOHN</i>	2015:306

SPEEDING UP MCMC BY DELAYED ACCEPTANCE AND DATA SUBSAMPLING <i>by MATIAS QUIROZ</i>	2015:307
Modeling financial sector joint tail risk in the euro area <i>by André Lucas, Bernd Schwaab and Xin Zhang</i>	2015:308
Score Driven Exponentially Weighted Moving Averages and Value-at-Risk Forecasting <i>by André Lucas and Xin Zhang</i>	2015:309
On the Theoretical Efficacy of Quantitative Easing at the Zero Lower Bound <i>by Paola Boel and Christopher J. Waller</i>	2015:310
Optimal Inflation with Corporate Taxation and Financial Constraints <i>by Daria Finocchiaro, Giovanni Lombardo, Caterina Mendicino and Philippe Weil</i>	2015:311
Fire Sale Bank Recapitalizations <i>by Christoph Bertsch and Mike Mariathasan</i>	2015:312
Since you're so rich, you must be really smart: Talent and the Finance Wage Premium <i>by Michael Böhm, Daniel Metzger and Per Strömberg</i>	2015:313
Debt, equity and the equity price puzzle <i>by Daria Finocchiaro and Caterina Mendicino</i>	2015:314
Trade Credit: Contract-Level Evidence Contradicts Current Theories <i>by Tore Ellingsen, Tor Jacobson and Erik von Schedvin</i>	2016:315
Double Liability in a Branch Banking System: Historical Evidence from Canada <i>by Anna Grodecka and Antonis Kotidis</i>	2016:316
Subprime Borrowers, Securitization and the Transmission of Business Cycles <i>by Anna Grodecka</i>	2016:317
Real-Time Forecasting for Monetary Policy Analysis: The Case of Sveriges Riksbank <i>by Jens Iversen, Stefan Laséen, Henrik Lundvall and Ulf Söderström</i>	2016:318
Fed Liftoff and Subprime Loan Interest Rates: Evidence from the Peer-to-Peer Lending <i>by Christoph Bertsch, Isaiah Hull and Xin Zhang</i>	2016:319
Curbing Shocks to Corporate Liquidity: The Role of Trade Credit <i>by Niklas Amberg, Tor Jacobson, Erik von Schedvin and Robert Townsend</i>	2016:320
Firms' Strategic Choice of Loan Delinquencies <i>by Paola Morales-Acevedo</i>	2016:321
Fiscal Consolidation Under Imperfect Credibility <i>by Matthieu Lemoine and Jesper Lindé</i>	2016:322
Challenges for Central Banks' Macro Models <i>by Jesper Lindé, Frank Smets and Rafael Wouters</i>	2016:323
The interest rate effects of government bond purchases away from the lower bound <i>by Rafael B. De Rezende</i>	2016:324
COVENANT-LIGHT CONTRACTS AND CREDITOR COORDINATION <i>by Bo Becker and Victoria Ivashina</i>	2016:325
Endogenous Separations, Wage Rigidities and Employment Volatility <i>by Mikael Carlsson and Andreas Westermark</i>	2016:326
Renovatio Monetae: Gesell Taxes in Practice <i>by Roger Svensson and Andreas Westermark</i>	2016:327
Adjusting for Information Content when Comparing Forecast Performance <i>by Michael K. Andersson, Ted Aranki and André Reslow</i>	2016:328
Economic Scarcity and Consumers' Credit Choice <i>by Marieke Bos, Chloé Le Coq and Peter van Santen</i>	2016:329
Uncertain pension income and household saving <i>by Peter van Santen</i>	2016:330
Money, Credit and Banking and the Cost of Financial Activity <i>by Paola Boel and Gabriele Camera</i>	2016:331
Oil prices in a real-business-cycle model with precautionary demand for oil <i>by Conny Olovsson</i>	2016:332
Financial Literacy Externalities <i>by Michael Haliasso, Thomas Jansson and Yigitcan Karabulut</i>	2016:333

The timing of uncertainty shocks in a small open economy <i>by Hanna Armelius, Isaiah Hull and Hanna Stenbacka Köhler</i>	2016:334
Quantitative easing and the price-liquidity trade-off <i>by Marien Ferdinandusse, Maximilian Freier and Annukka Ristiniemi</i>	2017:335
What Broker Charges Reveal about Mortgage Credit Risk <i>by Antje Berndt, Burton Hollifield and Patrik Sandås</i>	2017:336
Asymmetric Macro-Financial Spillovers <i>by Kristina Bluwstein</i>	2017:337
Latency Arbitrage When Markets Become Faster <i>by Burton Hollifield, Patrik Sandås and Andrew Todd</i>	2017:338
How big is the toolbox of a central banker? Managing expectations with policy-rate forecasts: Evidence from Sweden <i>by Magnus Åhl</i>	2017:339
International business cycles: quantifying the effects of a world market for oil <i>by Johan Gars and Conny Olovsson I</i>	2017:340
Systemic Risk: A New Trade-Off for Monetary Policy? <i>by Stefan Laséen, Andrea Pescatori and Jarkko Turunen</i>	2017:341
Household Debt and Monetary Policy: Revealing the Cash-Flow Channel <i>by Martin Flodén, Matilda Kilström, Jósef Sigurdsson and Roine Vestman</i>	2017:342
House Prices, Home Equity, and Personal Debt Composition <i>by Jieying Li and Xin Zhang</i>	2017:343
Identification and Estimation issues in Exponential Smooth Transition Autoregressive Models <i>by Daniel Buncic</i>	2017:344
Domestic and External Sovereign Debt <i>by Paola Di Casola and Spyridon Sichliris</i>	2017:345
The Role of Trust in Online Lending <i>by Christoph Bertsch, Isaiah Hull, Yingjie Qi and Xin Zhang</i>	2017:346
On the effectiveness of loan-to-value regulation in a multiconstraint framework <i>by Anna Grodecka</i>	2017:347
Shock Propagation and Banking Structure <i>by Mariassunta Giannetti and Farzad Saidi</i>	2017:348
The Granular Origins of House Price Volatility <i>by Isaiah Hull, Conny Olovsson, Karl Walentin and Andreas Westermark</i>	2017:349
Should We Use Linearized Models To Calculate Fiscal Multipliers? <i>by Jesper Lindé and Mathias Trabandt</i>	2017:350
The impact of monetary policy on household borrowing – a high-frequency IV identification <i>by Maria Sandström</i>	2018:351
Conditional exchange rate pass-through: evidence from Sweden <i>by Vesna Corbo and Paola Di Casola</i>	2018:352
Learning on the Job and the Cost of Business Cycles <i>by Karl Walentin and Andreas Westermark</i>	2018:353
Trade Credit and Pricing: An Empirical Evaluation <i>by Niklas Amberg, Tor Jacobson and Erik von Schedvin</i>	2018:354
A shadow rate without a lower bound constraint <i>by Rafael B. De Rezende and Annukka Ristiniemi</i>	2018:355
Reduced "Border Effects", FTAs and International Trade <i>by Sebastian Franco and Erik Frohm</i>	2018:356
Spread the Word: International Spillovers from Central Bank Communication <i>by Hanna Armelius, Christoph Bertsch, Isaiah Hull and Xin Zhang</i>	2018:357
Predictors of Bank Distress: The 1907 Crisis in Sweden <i>by Anna Grodecka, Seán Kenny and Anders Ögren</i>	2018:358

Diversification Advantages During the Global Financial Crisis <i>by Mats Levander</i>	2018:359
Towards Technology-News-Driven Business Cycles <i>by Paola Di Casola and Spyridon Sichliridis</i>	2018:360
The Housing Wealth Effect: Quasi-Experimental Evidence <i>by Dany Kessel, Björn Tyrefors and Roine</i>	2018:361
Identification Versus Misspecification in New Keynesian Monetary Policy Models <i>by Malin Adolfson, Stefan Laseén, Jesper Lindé and Marco Ratto</i>	2018:362
The Macroeconomic Effects of Trade Tariffs: Revisiting the Lerner Symmetry Result <i>by Jesper Lindé and Andrea Pescatori</i>	2019:363
Biased Forecasts to Affect Voting Decisions? The Brexit Case <i>by Davide Cipullo and André Reslow</i>	2019:364
The Interaction Between Fiscal and Monetary Policies: Evidence from Sweden <i>by Sebastian Ankargren and Hovick Shahnazarian</i>	2019:365
Designing a Simple Loss Function for Central Banks: Does a Dual Mandate Make Sense? <i>by Davide Debortoli, Jinill Kim and Jesper Lindé</i>	2019:366
Gains from Wage Flexibility and the Zero Lower Bound <i>by Roberto M. Billi and Jordi Galí</i>	2019:367
Fixed Wage Contracts and Monetary Non-Neutrality <i>by Maria Björklund, Mikael Carlsson and Oskar Nordström Skans</i>	2019:368
The Consequences of Uncertainty: Climate Sensitivity and Economic Sensitivity to the Climate <i>by John Hassler, Per Krusell and Conny Olovsson</i>	2019:369
Does Inflation Targeting Reduce the Dispersion of Price Setters' Inflation Expectations? <i>by Charlotte Paulie</i>	2019:370
Subsampling Sequential Monte Carlo for Static Bayesian Models <i>by David Gunawan, Khue-Dung Dang, Matias Quiroz, Robert Kohn and Minh-Ngoc Tran</i>	2019:371
Hamiltonian Monte Carlo with Energy Conserving Subsampling <i>by Khue-Dung Dang, Matias Quiroz, Robert Kohn, Minh-Ngoc Tran and Mattias Villani</i>	2019:372
Institutional Investors and Corporate Investment <i>by Cristina Cella</i>	2019:373
The Impact of Local Taxes and Public Services on Property Values <i>by Anna Grodecka and Isaiah Hull</i>	2019:374
Directed technical change as a response to natural-resource scarcity <i>by John Hassler, Per Krusell and Conny Olovsson</i>	2019:375
A Tale of Two Countries: Cash Demand in Canada and Sweden <i>by Walter Engert, Ben Fung and Björn Segendorf</i>	2019:376
Tax and spending shocks in the open economy: are the deficits twins? <i>by Mathias Klein and Ludger Linnemann</i>	2019:377
Mind the gap! Stylized dynamic facts and structural models <i>by Fabio Canova and Filippo Ferroni</i>	2019:378
Financial Buffers, Unemployment Duration and Replacement Labor Income <i>by Mats Levander</i>	2019:379
Inefficient Use of Competitors' Forecasts? <i>by André Reslow</i>	2019:380
How Much Information Do Monetary Policy Committees Disclose? Evidence from the FOMC's Minutes and Transcripts <i>by Mikael Apel, Marianna Blix Grimaldi and Isaiah Hull</i>	2019:381
Risk endogeneity at the lender/investor-of-last-resort <i>by Diego Caballero, André Lucas, Bernd Schwaab and Xin Zhang</i>	2019:382
Heterogeneity in Households' Expectations of Housing Prices – Evidence from Micro Data <i>by Erik Hjalmarsson and Pär Österholm</i>	2019:383
Big Broad Banks: How Does Cross-Selling A Affect Lending? <i>by Yingjie Qi</i>	2020:384
Unemployment Fluctuations and Nominal GDP Targeting <i>by Roberto Billi</i>	2020:385

FAQ: How do I extract the output gap? <i>by Fabio Canova</i>	2020:386
Drivers of consumer prices and exchange rates in small open economies <i>by Vesna Corbo and Paola Di Casola</i>	2020:387
TFP news, stock market booms and the business cycle: Revisiting the evidence with VEC models <i>by Paola Di Casola and Spyridon Sichelmiris</i>	2020:388
The costs of macroprudential deleveraging in a liquidity trap <i>by Jiaqian Chen, Daria Finocchiaro, Jesper Lindé and Karl Walentin</i>	2020:389
The Role of Money in Monetary Policy at the Lower Bound <i>by Roberto M. Billi, Ulf Söderström and Carl E. Walsh</i>	2020:390
MAJA: A two-region DSGE model for Sweden and its main trading partners <i>by Vesna Corbo and Ingvar Strid</i>	2020:391
The interaction between macroprudential and monetary policies: The cases of Norway and Sweden <i>by Jin Cao, Valeriya Dinger, Anna Grodecka-Messi, Ragnar Juelsrud and Xin Zhang</i>	2020:392
Withering Cash: Is Sweden ahead of the curve or just special? <i>by Hanna Armelius, Carl Andreas Claussen and André Reslow</i>	2020:393
Labor shortages and wage growth <i>by Erik Frohm</i>	2020:394
Macro Uncertainty and Unemployment Risk <i>by Joonseok Oh and Anna Rogantini Picco</i>	2020:395
Monetary Policy Surprises, Central Bank Information Shocks, and Economic Activity in a Small Open Economy <i>by Stefan Laséen</i>	2020:396
Econometric issues with Laubach and Williams' estimates of the natural rate of interest <i>by Daniel Buncic</i>	2020:397
Quantum Technology for Economists <i>by Isaiah Hull, Or Sattath, Eleni Diamanti and Göran Wendin</i>	2020:398



Sveriges Riksbank
Visiting address: Brunkebergs torg 11
Mail address: se-103 37 Stockholm

Website: www.riksbank.se
Telephone: +46 8 787 00 00, Fax: +46 8 21 05 31
E-mail: registratorn@riksbank.se